Molecular Biology of the Cell
Vol. 15, 5075–5091, November 2004

Role of Vma21p in Assembly and Transport of the Yeast Vacuolar ATPase

Per Malkus,* Laurie A. Graham,† Tom H. Stevens,† and Randy Schekman*‡

*Department of Molecular and Cell Biology, Howard Hughes Medical Institute, University of California, Berkeley, CA 94720; and †Institute of Molecular Biology, University of Oregon, Eugene, OR 97403

Submitted June 23, 2004; Accepted August 20, 2004
Monitoring Editor: Juan S. Bonifacino

The *Saccharomyces cerevisiae* vacuolar H^+-ATPase (V-ATPase) is a multisubunit complex composed of a peripheral membrane sector (V_1) responsible for ATP hydrolysis and an integral membrane sector (V_0) required for proton translocation. Biogenesis of V_0 requires an endoplasmic reticulum (ER)-localized accessory factor, Vma21p. We found that in *vma21*Δ cells, the major proteolipid subunit of V_0 failed to interact with the 100-kDa V_0 subunit, Vph1p, indicating that Vma21p is necessary for V_0 assembly. Immunoprecipitation of Vma21p from wild-type membranes resulted in coimmunoprecipitation of all five V_0 subunits. Analysis of *vma*Δ strains showed that binding of V_0 subunits to Vma21p was mediated by the proteolipid subunit Vma11p. Although Vma21p/proteolipid interactions were independent of Vph1p, Vma21p/Vph1p association was dependent on all other V_0 subunits, indicating that assembly of V_0 occurs in a defined sequence, with Vph1p recruitment into a Vma21p/proteolipid/Vma6p complex representing the final step. An in vitro assay for ER export was used to demonstrate preferential packaging of the fully assembled Vma21p/proteolipid/Vma6p/Vph1p complex into COPII-coated transport vesicles. Pulse-chase experiments showed that the interaction between Vma21p and V_0 was transient and that Vma21p/V_0 dissociation was concomitant with V_0/V_1 assembly. Blocking ER export in vivo stabilized the interaction between Vma21p and V_0 and abrogated assembly of V_0/V_1. Although a Vma21p mutant lacking an ER-retrieval signal remained associated with V_0 in the vacuole, this interaction did not affect the assembly of vacuolar V_0/V_1 complexes. We conclude that Vma21p is not involved in regulating the interaction between V_0 and V_1 sectors, but that it has a crucial role in coordinating the assembly of V_0 subunits and in escorting the assembled V_0 complex into ER-derived transport vesicles.

INTRODUCTION

Acidification of vacuoles/lysosomes, endosomes, and clathrin-coated vesicles is largely accomplished by the action of vacuolar-type proton-translocating ATPases (V-ATPases). Defects in V-ATPase function result in disruption of many cellular processes, including receptor-mediated endocytosis, targeting of lysosomal enzymes, zymogen activation, and uptake of small molecules through secondary transporters (Inoue *et al.*, 2003). The *Saccharomyces cerevisiae* V-ATPase is the most well-characterized member of this ubiquitous family of electrogenic pumps and is an excellent model for studying the biosynthesis of a multisubunit enzyme complex. The basic structure of V-ATPases is similar to mitochondrial F_0F_1-ATPases, consisting of an integral membrane V_0 sector and a peripherally associated V_1 sector. The V_0 sector is composed of multiple transmembrane proteins that form a pathway for proton translocation, whereas the cytosolic V_1 sector is assembled from soluble components that perform the catalytic functions of the enzyme. Genetic and biochemical analyses in yeast have identified 13 *VMA* (vacuolar membrane ATPase) genes that encode structural subunits of the V_0/V_1 complex.

Studies of *vma* mutants have revealed that V-ATPase assembly is in some ways a coordinated process (requiring the presence of other subunits) and is in other respects an autonomous process (proceeding in the absence of other V_0 or V_1 components). The cytosolic V_1 sector is composed of at least eight subunits (69, 60, 54, 42, 32, 27, 14, and 13 kDa). With the exception of cells lacking Vma4p or Vma10p, the loss of a V_1 subunit does not affect the stability of the remaining subunits, nor does it prevent their assembly into a V_1 substructure (Tomashek *et al.*, 1997). However, with one exception, loss of Vma13p, these partially assembled V_1 complexes fail to be recruited to the vacuolar membrane (Ho *et al.*, 1993b). In cells lacking any one of the five gene products (100, 36, 23, 17, and 16 kDa) comprising the V_0 sector, the V_1 sector also fails to be recruited to the membrane (Bauerle *et al.*, 1993; Hirata *et al.*, 1997; Graham *et al.*, 2003).

V_0 subunits are assembled and delivered to the vacuole independently of V_1; however, the assembly and stability of V_0 subunits is severely compromised in the absence of any of the other V_0 components. Notably, the stability of the 100-kDa subunit, Vph1p, is drastically reduced in cells lacking other V_0 subunits (Graham *et al.*, 1998). The half-time for Vph1p turnover is greater than 400 min in wild-type cells, compared with ~30 min in V_0 mutants. Several lines of evidence indicate that Vph1p molecules that fail to assemble into V_0 are degraded directly out of the endoplasmic reticulum (ER) via a proteasomal pathway (Hill and Stevens, 1995; Hill and Cooper, 2000; Wilhovsky *et al.*, 2000). The 36-kDa subunit (Vma6p) is a peripheral membrane protein that remains stable in V_0 mutants but no longer associates with membranes. The highly hydrophobic 16-, 17-, and 23-kDa subunits (Vma11p, Vma3p, and Vma16p, respectively),

Article published online ahead of print. Mol. Biol. Cell 10.1091/mbc.E04–06–0514. Article and publication date are available at www.molbiolcell.org/cgi/doi/10.1091/mbc.E04–06–0514.

‡ Corresponding author. E-mail address: schekman@berkeley.edu.

Table 1. Yeast strains and plasmids used in this study

Strain	Genotype	Source/Reference
SF838	*MATα ura3-52 leu2-3,112 his4-579 ade6 pep4-3*	Rothman and Stevens, 1986
KHY3	*MATα ura3-52 leu2-3,112 his4-579 ade6 pep4-3 vma21Δ::LEU2*	Hill and Stevens, 1994
LGY17	*MATα ura3-52 leu2-3,112 his4-579 ade6 pep4-3 vma12Δ::LEU2*	Jackson and Stevens, 1997
KHY34	*MATα ura3-52 leu2-3,112 his4-579 ade6 pep4-3 vma22Δ::LEU2*	Hill and Stevens, 1995
KHY31	*MATα ura3-52 leu2-3,112 his4-579 ade6 pep4-3 vph1Δ::LEU2*	Graham *et al.*, 1998
vma3Δ-1	*MATα ura3-52 leu2-3,112 his4-579 ade6 pep4-3 vma3Δ::URA3*	Kane *et al.*, 1992
RHA107	*MATα ura3-52 leu2-3,112 his4-579 ade6 pep4-3 vma11Δ::LEU2*	Graham *et al.*, 1998
LGY9	*MATα ura3-52 leu2-3,112 his4-579 ade6 pep4-3 vma16Δ::LEU2*	Graham *et al.*, 1998
CBY1	*MATα ura3-52 leu2-3,112 his4-579 ade6 pep4-3 vma6Δ::LEU2*	Bauerle *et al.*, 1993
RHY374	*MATα ura3-52 leu2-3,112 his4-579 ade6 pep4-3 VMA3::HA::URA3*	Hirata *et al.*, 1997
PMY78	*MATα ura3-52 leu2-3,112 his4-579 ade6 pep4-3 vma21Δ::LEU2 VMA3::HA::URA3*	This study
PMY79	*MATα ura3-52 leu2-3,112 his4-579 ade6 pep4-3 vma12Δ::LEU2 VMA3::HA::URA3*	This study
PMY80	*MATα ura3-52 leu2-3,112 his4-579 ade6 pep4-3 vma22Δ::LEU2 VMA3::HA::URA3*	This study
PMY81	*MATα ura3-52 leu2-3,112 his4-579 ade6 pep4-3 vph1Δ::LEU2 VMA3::HA::URA3*	This study
PMY82	*MATα ura3-52 leu2-3,112 his4-579 ade6 pep4-3 vma11Δ::LEU2 VMA3::HA::URA3*	This study
PMY83	*MATα ura3-52 leu2-3,112 his4-579 ade6 pep4-3 vma16Δ::LEU2 VMA3::HA::URA3*	This study
PMY84	*MATα ura3-52 leu2-3,112 his4-579 ade6 pep4-3 vma6Δ::LEU2 VMA3::HA::URA3*	This study
RSY250	*MATα ura3-52*	D. Botstein
RSY263	*MATα ura3-52 sec12-4*	Novick *et al.*, 1980
RSY271	*MATα ura3-52 his4-619 sec18-1*	Kaiser and Schekman, 1990

Plasmid	Description	Source/Reference
pKH28	*VMA21::HA* in pRS316	Hill and Stevens, 1994
pLG42	*VMA21::HA* in pRS315	This study
pKH31	*vma21(QQ)::HA* in pRS316	Hill and Stevens, 1994
pDJ12	*VMA12::HA* in pRS316	Jackson and Stevens, 1997
pRHA318	*VMA3::HA::URA3* in pRS314	Gift of R. Hirata
pRHA316	*VMA3::c-myc::URA3* in pRS314	Gift of R. Hirata
pLG33	*VMA16::c-myc* in pRS316	Powell *et al.*, 2000
pLG37	*VMA11::c-myc* in pRS316	Powell *et al.*, 2000

termed proteolipids, have been difficult to characterize biochemically (Hirata *et al.*, 1997).

Genetic screens for *vma* mutants have also led to the isolation of three genes, *VMA12, VMA21*, and *VMA22*, that are required for V-ATPase biogenesis, but whose products are not structural components of V_0V_1 (Bachhawat *et al.*, 1993; Ho *et al.*, 1993a; Hill and Stevens, 1994). The biochemical phenotypes of *vma12*Δ, *vma22*Δ, and *vma21*Δ cells resemble those of strains lacking a structural subunit of V_0: V_0 fails to assemble properly, V_0 subunits are not transported to the vacuole, and Vph1p is rapidly degraded via a proteasomal pathway (Hill and Stevens, 1995; Hill and Cooper, 2000; Wilhovsky *et al.*, 2000). Interestingly, immunofluorescence and cell fractionation studies showed that all three proteins localize to the ER, suggesting that they have a dedicated role in V_0 biogenesis (Hill and Stevens, 1994, 1995; Jackson and Stevens, 1997; Graham *et al.*, 2003).

Vma12p is a 25-kDa integral membrane protein predicted to contain two transmembrane segments (Jackson and Stevens, 1997). Vma22p is a 21-kDa peripheral membrane protein whose membrane association is dependent on Vma12p (Hill and Stevens, 1995). Indeed, Vma12p and Vma22p interact to form an assembly complex that binds newly synthesized Vph1p molecules in the ER (Graham *et al.*, 1998). Neither Vma21p nor other V_0 subunits were found associated with the Vma12/22p assembly complex. Furthermore, the interaction between Vma12/22p and Vph1p persisted in *vma21*Δ cells and in cells lacking any one of the proteolipid subunits of V_0 (Graham *et al.*, 1998). Together these findings suggest that Vma12/22p is dedicated to Vph1p maturation/assembly and that Vma21p might act at a subsequent stage in V_0 assembly or in a parallel pathway.

VMA21 encodes an 8.5-kDa integral membrane protein that is predicted to span the membrane twice with both the amino- and carboxy-termini facing the cytosol. Intriguingly, the carboxy-terminus of Vma21p contains a −KKXX ER-retrieval sequence. Mutation of the −KKXX motif in Vma21p to −QQXX led to the mislocalization of Vma21(QQ)p to the vacuolar membrane (Hill and Stevens, 1994). This observation suggests that Vma21p cycles between the ER and Golgi and that it may have a role in the transport of V_0 subcomplex out of the ER. Interestingly, despite Vma21(QQ)p being mislocalized to the vacuole, Vma21(QQ)p is able to function in the assembly of the V-ATPase. Vacuoles prepared from *vma21*Δ cells expressing Vma21(QQ)p retain 30% of wild-type V-ATPase activity (Hill and Stevens, 1994). These data indicate that Vma21p is required for V_0 assembly and suggest that ER retrieval is important for Vma21p to act in multiple rounds of assembly.

In this article we use biochemical tools to further characterize the role of ER-localized accessory factors in V_0 biogenesis. We found that Vma12p/Vma22p were not required for interaction of V_0 subunits, but were essential for the productive assembly of these subunits into a functional V_0 structure. In contrast, Vma21p was found to be required for the association of V_0 subunits and was enriched as a complex with V_0 during COPII vesicle formation.

MATERIALS AND METHODS

Yeast Strains, Growth Conditions, and Reagents

Yeast strains and plasmids used in this study are listed in Table 1. Yeast were transformed using a standard lithium acetate procedure (Schiestl and Gietz, 1989). Yeast were grown in minimal (SD) or rich (YPD) medium (Sherman,

1991) at 30°C or at 24°C for temperature sensitive strains. Vma$^-$ strains were grown in SD medium or in YPD that was buffered at pH 5 with 50 mM succinate/phosphate (Kane *et al.*, 1992).

Rabbit polyclonal antibodies raised against a 12× HA epitope (Bowers *et al.*, 2000) and against a maltose-binding protein (MBP) fusion to the N-terminal cytosolic domain (a.a. 1–369) of Vph1p (Hill and Stevens, 1994) were generated as described. Purified mouse monoclonal antibodies against HA (HA.11) were obtained from BAbCo (Berkeley, CA). Mouse monoclonal antibodies against Vph1p (10D7), Vma1p (8B1), and Vma2p (13D11) were purchased from Molecular Probes (Eugene, OR). Rabbit polyclonal antibodies against CPY (Stevens *et al.*, 1982) and against Chs3p (Chuang and Schekman, 1996) were also used in these experiments.

Metabolic Labeling and Pulse-chase Analysis

Yeast cells were grown to midlog phase, harvested, washed twice with SD media, and then grown in the absence of methionine for 15 min. [^{35}S]methionine/[^{35}S]cysteine labeling mix (^{35}S-Promix, Amersham Biosciences, Piscataway, NJ) was added (6 μCi for each OD_{600} of cells harvested) and growth was continued for 3–60 min. Labeling was terminated by the addition of chase mix containing excess unlabeled amino acids (Chuang and Schekman, 1996). Samples removed at various times during the chase period were arrested by the addition of sodium azide to 20 mM and incubation on ice. When all time points had been collected, cells were harvested by centrifugation and converted to spheroplasts with lyticase (Wuestehube and Schekman, 1992).

Pulse-chase experiments designed to preserve the interaction between V_0 and V_1 were conducted using spheroplasts, as described in Kane (1995).

Immunoprecipitations

For denaturing immunoprecipitations, 100 μl 1% SDS was added to sedimented spheroplasts. Samples were heated at 55°C for 5–10 min and 1 ml of dilution buffer (50 mM Tris-HCl, pH 7.5, 150 mM NaCl, 1% Triton X-100, 2 mM NaN_3) containing protease inhibitors (1 mM PMSF, 1 μg/μl leupeptin, 1 μg/μl pepstatin, 2 μg/μl chymostatin, 5 μg/μl aprotinin) was added. Samples were placed on ice for ~10 min, and insoluble material was removed by centrifugation. Antibodies precoupled to either protein A- (Amersham Biosciences) or protein G-Sepharose (Sigma-Aldrich, St. Louis, MO) were added and mixed with membrane extracts for either 2 h at room temperature or overnight at 4°C. Immune complexes were washed three times with dilution buffer containing 0.1% SDS, once with Tris/NaCl (10 mM Tris-HCl, pH 7.5, 50 mM NaCl, 2 mM NaN_3), and eluted with 2× sample buffer (2× SB; Ausubel *et al.*, 1987) with heating at 55°C for 10 min.

For nondenaturing immunoprecipitations, 1 ml of 1% $C_{12}E_9$ (Sigma-Aldrich) in PBS (containing protease inhibitors as described for dilution buffer) was used to solubilize sedimented spheroplasts. Protein A-Sepharose (50 μl) was added, and samples were mixed for 30 min at 4°C. Insoluble material was removed by centrifugation (12,000 × *g*, 15 min, 4°C) and immobilized antibody was incubated with the soluble material at 4°C for >4 h to overnight. Unbound material was removed by washing four times with 1% $C_{12}E_9$ in PBS and once with Tris/NaCl. Immune complexes were eluted with 2× SB and heating and analyzed by SDS-PAGE and phosphorimaging.

Nondenaturing immunoprecipitation of Vma1p was carried out as described in Kane (1995) using monoclonal antibodies against Vma1p. Nondenaturing immunoprecipitation of Vma21p(QQ)-HA from solubilized vacuolar membranes was carried out as previously described by Powell *et al.* (2000) using rabbit anti-HA sera.

In Vitro Assay for ER Export via COPII-coated Vesicles

Semi-intact yeast cells (SICs) and yeast microsomal membranes used in COPII packaging assays were prepared as described (Shimoni and Schekman, 2002). COPII-coated vesicle packaging assays were performed as described in Kuehn *et al.* (1996). Antibody inhibition experiments were performed as follows: SICs were sedimented, resuspended in 1 ml high acetate B88 (1 M KOAc, 20 mM HEPES-KOH, pH 6.8, 250 mM sorbitol, 5 mM $Mg(OAc)_2$) and incubated on ice for 5 min. They were then washed twice with B88 (150 mM KOAc, 20 mM HEPES-KOH, pH 6.8, 250 mM sorbitol, 5 mM $Mg(OAc)_2$) and brought to 50 OD/ml. Bovine serum albumin (BSA; Two hundred microliters of a 10% solution in B88) was added to the membranes before the addition of 10 μg of monoclonal antibodies against HA. Mock incubations were conducted in parallel and differed only in that anti-HA antibodies were omitted. Samples were mixed at 4°C for 90 min, and then unbound antibodies were removed by washing twice with 0.1% BSA in B88 and twice with B88. Membranes were then used in COPII-coated vesicle packaging assays.

Glycerol Gradient Fractionation of Vacuolar Membranes

Vacuolar membranes were prepared from *vma21*Δ cells expressing either Vma21p-HA (pKH28) or Vma21p(QQ)-HA (pKH31) as previously described (Conibear and Stevens, 2002). Vacuolar membranes were resuspended in TE + 10% glycerol to a protein concentration of 5 mg/ml and solubilized with 1% C12E9 (final concentration). Solubilized proteins were fractionated on a 12.5 ml 20–50% glycerol gradient poured in tubes for a SW41 rotor after centrifugation at 175,000 × *g* for 20 h (Kane *et al.*, 1989). Fractions of ~0.75 ml were removed from the top of the gradient, analyzed by SDS-PAGE, and probed with antibodies specific to Vph1p, Vma2p, and HA.

RESULTS

Vma21p Is Required for V_0 Assembly

Previous work has shown that Vph1p is rapidly degraded in cells lacking any one of the ER-localized accessory factors (*vma12*Δ, *vma21*Δ, or *vma22*Δ) required for V_0 biogenesis (Hill and Stevens, 1994, 1995; Jackson and Stevens, 1997). We speculated that in the absence of accessory factors, V_0 subunits would fail to associate with each other, resulting in free Vph1p molecules being diverted for degradation. To test this, we assessed the interaction between Vph1p and the major proteolipid subunit of V_0, Vma3p, by coimmunoprecipitation.

A fully functional *VMA3::HA* allele was integrated at the *VMA3* locus in wild-type and *vma*Δ strains (Hirata *et al.*, 1997). Transformants that expressed Vma3p-HA were grown to midlog phase and metabolically labeled with [^{35}S]methionine for 60 min. Half of the cell extract was solubilized under denaturing conditions and used in immunoprecipitations with anti-Vph1p antibodies (Figure 1, Vph, odd numbered lanes). The remaining half was solubilized under nondenaturing conditions using a detergent ($C_{12}E_9$) known to preserve interactions within the fully assembled V_0 complex (Doherty and Kane, 1993). Immunoprecipitations with anti-HA antibodies were performed to recover Vma3p-HA (Figure 1, HA, even numbered lanes), and the amount of coimmunoprecipitated 100-kDa subunit was compared with that found in anti-Vph1p immunoprecipitations.

Two control experiments presented in Figure 1 confirmed the specificity of the immunoprecipitations. In cells lacking HA-tagged Vma3p (lane 2), Vph1p was not directly recovered by anti-HA antibodies, as demonstrated by the absence of a 100-kDa band in anti-HA immunoprecipitations. Second, no significant 100-kDa band was detected in immunoprecipitations from *vph1*Δ cell extracts (lanes 5 and 6). This demonstrates two important points: that our Vph1p antibody does not recognize the alternative 100-kDa subunit, Stv1p; and that Stv1p is not a significant component of the 100-kDa band recovered in complex with Vma3p-HA. This is consistent with the fact that Stv1p is expressed at much lower levels than Vph1p and represents only a small fraction of total cellular 100-kDa V_0 subunit (Manolson *et al.*, 1994).

Analysis of wild-type *VMA3::HA* cells showed that a prominent 100-kDa band was coimmunoprecipitated with Vma3p-HA (Figure 1, lanes 3 and 4). Quantification of these results revealed that ~80% of radiolabeled Vph1p was coimmunoprecipitated with Vma3p-HA. This indicates that the majority of Vph1p synthesized during the 60-min labeling period assembled into a V_0 structure in Vma$^+$ cells. In contrast, immunoprecipitations from cells lacking a proteolipid subunit of V_0 (*vma11*Δ) showed that only ~2.6% of radiolabeled Vph1p was recovered in a complex with Vma3p-HA (Figure 1, lanes 7 and 8). Similar results were obtained in *vma6*Δ cells (Figure 1, lanes 9 and 10), where ~1.1% of Vph1p coimmunoprecipitated with Vma3p-HA, and in *vma16*Δ cells (unpublished data). Thus, Vph1p fails to interact with Vma3p if any one of the other three structural subunits of V_0 is absent. This finding supports the idea that Vph1p requires association with other V_0 subunits for its stability.

We next asked whether ER-accessory factors are required to facilitate the association of V_0 subunits. In *VMA3::HA*

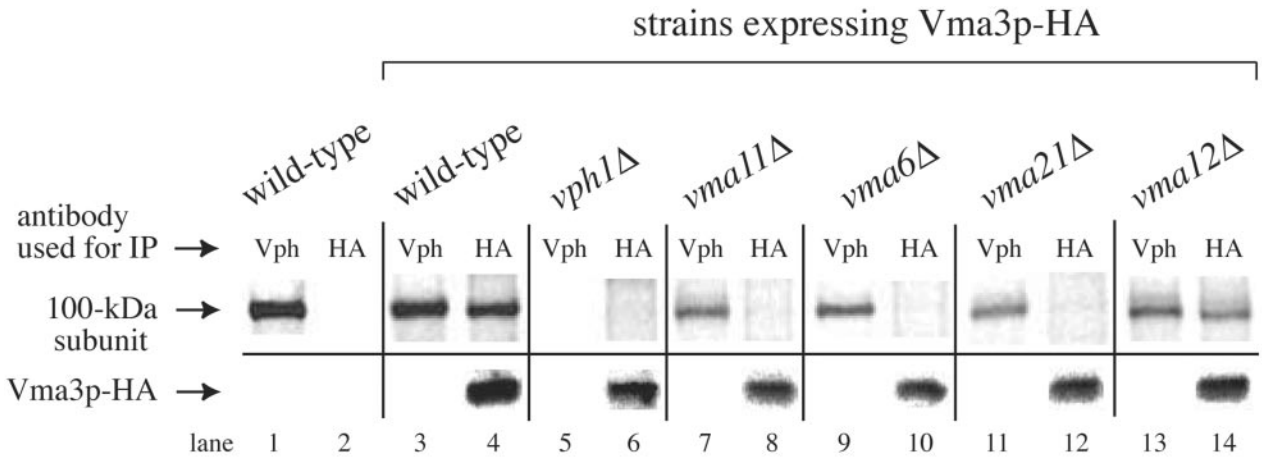

Figure 1. Vma21p is required for V_0 assembly. Wild-type and *vma*Δ strains transformed with an HA-tagged version of the major proteolipid V_0 subunit (*VMA3::HA*) were metabolically labeled with [^{35}S]methionine for 60 min and harvested. Control cells lacking the HA-tagged *VMA3* allele were treated similarly. Whole cell membrane extracts were prepared and split into two equal size samples. One aliquot was solubilized in 1% SDS (denaturing conditions) and used for immunoprecipitations with antibodies against Vph1p. The other was solubilized in 1% $C_{12}E_9$ (nondenaturing conditions) and mixed with Sepharose-bound anti-HA antibodies to recover Vma3p-HA. Immunoprecipitated proteins were separated by SDS-PAGE and analyzed with a phosphorimager.

*vma21*Δ cells, Vph1p failed to coimmunoprecipitate with Vma3p-HA, indicating that Vma21p is required for V_0 assembly (Figure 1, lanes 11 and 12). Unexpectedly, we found that in *vma12*Δ cells, Vph1p was efficiently coimmunoprecipitated with Vma3p-HA (Figure 1, lanes 13 and 14). Approximately 70% of radiolabeled Vph1p in *vma12*Δ cells was complexed with Vma3p-HA. Identical results were observed in *vma22*Δ cells (unpublished data). Previous work has shown that Vma12p/Vma22p interacts with Vph1p during its biogenesis and that this interaction is required for Vph1p stability (Graham *et al.*, 1998). However, our findings indicate that Vph1p still interacts with other V_0 subunits in the absence of Vma12p/Vma22p, but that this interaction is not sufficient to guard Vph1p from degradation.

Vma21p Interacts with V_0 Subunits

The results from Figure 1 indicated that Vma21p plays a critical role in bringing together Vph1p and the proteolipid subunits of the V_0 complex. To better understand how Vma21p facilitates this process, we asked whether Vma21p itself interacted with V_0 subunits. The Vma12p/Vma22p complex is known to bind directly to Vph1p during V_0 biogenesis, so we speculated that Vma21p might associate with the proteolipid subunits of V_0 in a parallel pathway (Graham *et al.*, 1998).

To address this question, we took a similar strategy to that outlined for the experiments in Figure 1. Cells expressing a functional, HA-tagged version of Vma21p were radiolabeled with [^{35}S]methionine for 20 min, membranes were solubilized under nondenaturing conditions, and Vma21p-HA was recovered by immunoprecipitation with antibodies against HA. Immunoprecipitated proteins were separated by SDS-PAGE and analyzed with a phosphorimager. The control experiment shown in lane 1 of Figure 2A, demonstrated that only a few radiolabeled proteins were nonspecifically immunoprecipitated from cells that lacked an HA-tagged protein. In contrast, immune complexes isolated from wild-type cells expressing Vma21p-HA contained a number of prominent radiolabeled proteins (Figure 2A, lane 2). The ~14-kDa protein at the bottom of the gel was identified as Vma21p-HA by performing anti-HA immunoprecipitations under denaturing conditions (unpublished data). Seven coimmunoprecipitated proteins were clearly present in immune complexes isolated from cells expressing Vma21p-HA and absent from the control sample (bands present in Figure 2A, lane 2 and not in lane 1). The electrophoretic mobility of five of these proteins corresponds exactly to the previously reported mobility of the five structural subunits of V_0 (Vph1p, 100-kDa; Vma6p, 36-kDa; Vma16p, 23-kDa; Vma3p, 17-kDa; Vma11p, 16-kDa; Hirata *et al.*, 1997). We confirmed the identity of these V_0 subunits by secondary immunoprecipitation using antibodies against Vph1p (unpublished data) and by analysis of *vma*Δ strains (Figure 2A, lanes 3–7). To identify conclusively the three proteolipid species, we repeated the experiment described in Figure 2A using strains that express myc-tagged versions of Vma3p, Vma11p, and Vma16p. Addition of the myc-tag resulted in a shift in electrophoretic mobility that allowed us to clearly resolve each proteolipid species in Vma21p-HA immune complexes (Figure 2B). In addition to the five V_0 subunits, two other prominent radiolabeled species were detected in Vma21p-HA immune complexes (Figure 2A, asterisks). The identity of these proteins was not determined, but their electrophoretic mobility does not correspond to that of Vma12p or Vma22p (Hirata *et al.*, 1993; Hill and Stevens, 1995).

Having found that all five structural components of V_0 associate with Vma21p-HA, we wondered whether Vma21p interacts directly or indirectly with individual subunits. Therefore, we examined which V_0 subunits coimmunoprecipitated with Vma21p-HA in a series of *vma*Δ strains (Figure 2A, lanes 3–7). In *vph1*Δ cells expressing Vma21p-HA, only the 100-kDa band corresponding to Vph1p was absent from the collection of proteins immunoprecipitated from wild-type cells (compare lanes 2 and 3 in Figure 2A). Deletion of any of the other four structural components of V_0 (*vma6*Δ, *vma16*Δ, *vma3*Δ, and *vma11*Δ, Figure 2A, lanes 4–7) also resulted in loss of Vph1p from Vma21p-HA immune complexes. Although Vph1p is destabilized in these strain backgrounds, resulting in reduced levels of total radiolabeled Vph1p (Figure 1, lanes 7–14), this instability cannot account for the absence of a significant 100-kDa band in

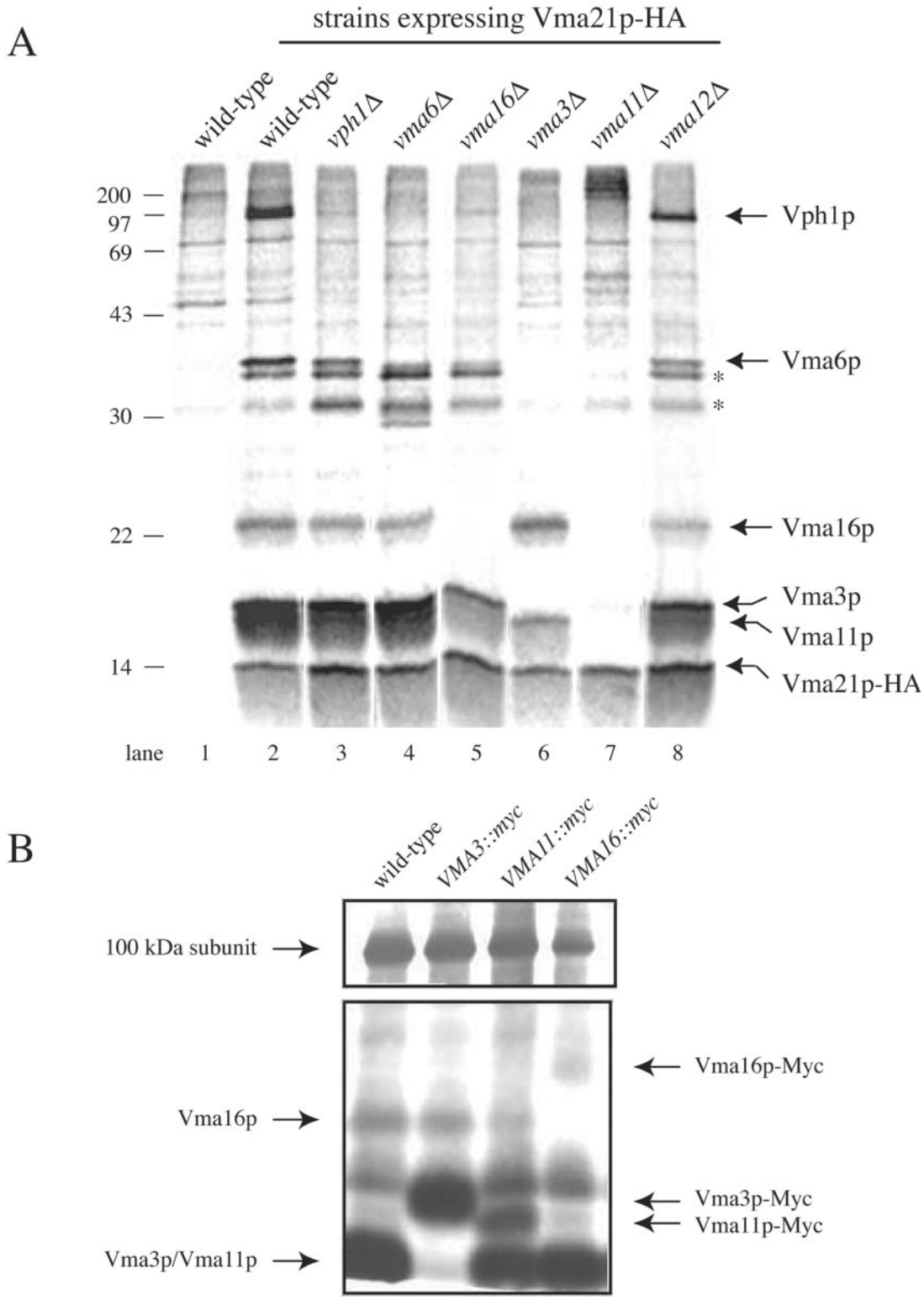

Figure 2. Vma21p interacts with V_0 subunits. (A) Wild-type and *vma*Δ strains expressing Vma21p-HA were metabolically labeled with [^{35}S]methionine for 20 min. Control strains possessing an untagged *VMA21* allele were treated similarly. Cells were lysed and membranes were solubilized in 1% $C_{12}E_9$ (nondenaturing conditions). Sepharose-coupled anti-HA antibodies were used to immunoprecipitate Vma21p-HA from the detergent extract. Bound material was resolved by SDS-PAGE (15% gel) and analyzed with a phosphorimager. Molecular-weight markers (kDa) are marked to the left. Two bands of unknown identity that are found specifically in immunoprecipitations from strains harboring *VMA21-HA* are marked with asterisks. (B) Yeast cells expressing plasmid-borne Vma21p-HA and integrated c-myc–tagged versions of either Vma3p, Vma11p, or Vma16p were labeled, lysed, and solubilized. Vma21p-HA immune complexes were recovered and analyzed as described in Figure 2A. The epitope-tagged proteins can be identified by their shift in size (lanes 2–4) when compared with the untagged versions of the proteins (lane 1).

Figure 2A, lanes 4–7. Therefore, the interaction between Vma21p and Vph1p appears to be very indirect, requiring that all other V_0 subunits are present. Together with our observation that Vph1p fails to interact with Vma3p-HA in *vma11*Δ, *vma16*Δ, and *vma6*Δ cells (Figure 1 and unpublished data), we conclude that Vph1p is only incorporated into a nascent V_0 structure when all other V_0 subunits are preassembled in a complex with Vma21p.

As mentioned above, in *vma6*Δ cells expressing Vma21p-HA, the 100-kDa band corresponding to Vph1p was not detected in anti-HA immune complexes. As expected, the band at ~36-kDa corresponding to Vma6p, was also absent (Figure 2A, lane 4). However, all three proteolipid subunits were recovered along with Vma21p-HA in *vma6*Δ cells.

Analysis of strains lacking individual proteolipid subunits is shown in lanes 5–7 of Figure 2A. In all three proteolipid mutants, the Vph1p and Vma6p failed to coimmunoprecipitate with Vma21p-HA. This indicates that, akin to Vph1p, recruitment of Vma6p into V_0 requires a preassembled Vma21p/proteolipid complex. In *vma16*Δ cells, we also failed to detect the 23-kDa subunit (Vma16p), but still observed coimmunoprecipitation of the Vma3p (17-kDa), and perhaps also Vma11p (16-kDa; obscured by smearing of the 17-kDa band; Figure 2A, lane 5). Similarly, the Vma16p and Vma11p were recovered in a complex with Vma21p-HA in the absence of Vma3p (Figure 2A, lane 6). However, in *vma11*Δ cells, Vma21p-HA did not coimmunoprecipitate any of the other V_0 subunits, indicating that Vma11p is likely to provide the sole binding surface that allows Vma21p-HA to interact with other V_0 subunits (Figure 2A, lane 7).

The experiment in Figure 1 yielded the unexpected result that Vph1p can interact with the major proteolipid subunit of V_0 (Vma3p) in *vma12*Δ cells. Consistent with this observation, we found that all five V_0 subunits were present in Vma21p-HA immune complexes isolated from *vma12*Δ cells (Figure 2A, lane 8). Identical results were obtained in *vma22*Δ cells (unpublished data). These results demonstrate that all five V_0 subunits associate in *vma12*Δ and *vma22*Δ mutants, forming a complex whose composition is identical to that observed in wild-type cells, but whose structure or organization is aberrant.

Vma21p/V_0 Association Is Transient and Is Stabilized by Blocking Exit from the ER

Vma21p is localized to the ER at steady state, whereas Vph1p and other V_0 subunits are most abundant in the vacuolar membrane. Therefore, the interaction between Vma21p and V_0 should be transient, occurring only during V_0 biogenesis. We explored the dynamics of the association between Vma21p and the V_0 complex using a pulse-chase protocol.

Cells expressing Vma21p-HA were grown overnight at 24°C, and then 5 min before labeling, cultures were split and incubated at either 24 or 37°C. Pulse labeling was initiated by the addition of [^{35}S]methionine, and 5 min later terminated by the addition of an excess of nonradioactive amino acids. Aliquots of cells collected at various times during the chase period were solubilized under nondenaturing conditions. Anti-HA immune complexes isolated from these cell extracts were resolved by SDS-PAGE and analyzed using a phosphorimager. Vph1p that coimmunoprecipitated with Vma21p-HA is shown in Figure 3A. We inferred the kinetics of Vma21p/V_0 interactions from coimmunoprecipitation of Vph1p with Vma21p. This simplification is justified from the experiments in Figure 2A, which demonstrated Vph1p only interacts with Vma21p when all other V_0 subunits are bound to Vma21p. Therefore, coimmunoprecipitation of Vph1p represents coimmunoprecipitation of the V_0 sector.

The top panel of Figure 3A shows that in wild-type cells incubated at either 24 or 37°C, the amount of Vph1p complexed with Vma21p-HA decreases over the course of the chase. The kinetics of Vma21p/Vph1p dissociation are rapid, with only half of radiolabeled Vph1p recovered in complex with Vma21p-HA after 5.4 min of chase (Figure 3B). As might be expected, the kinetics of Vma21p/V_0 dissociation is faster at 37°C ($t_{1/2} \approx 3.0$ min). The decrease in the amount Vph1p coimmunoprecipitated with Vma21p-HA was not a result of Vph1p degradation, because no significant change was observed in the total amount of radiolabeled Vph1p present in cells during the 16-min chase period (unpublished data).

We extended this analysis by exploring the dynamics of Vma21p/V_0 association in a *sec12-4* strain that displays a conditional defect in the budding of secretory vesicles from the ER (Kaiser and Schekman, 1990). The bottom panel of Figure 3A shows that Vph1p dissociated from Vma21p-HA in *sec12−4* cells held at 24°C, but remained associated with Vma21p-HA when *sec12−4* cells were incubated at 37°C. The graph in Figure 3B is a quantification of the data presented in Figure 3A.

These experiments demonstrated that the Vma21p/V_0 complex we identified was not an artifact that occurs after cell lysis and loss of compartmental integrity. Rather, as radiolabeled Vph1p molecules moved through the secretory pathway to the vacuole, the interaction between Vma21p and Vph1p was lost. Furthermore, blocking transport from the ER prolonged the interaction between Vma21p and V_0, suggesting that Vma21p may dissociate from the assembled V_0 complex only after exiting the ER. The notion that Vma21p normally leaves the ER is supported by the presence of a bona fide ER-retrieval motif in its C-terminal cytosolic domain (Hill and Stevens, 1994). We next entertained the possibility that Vma21p promotes packaging of the assembled V_0 complex into COPII-coated transport vesicles, which carry secretory cargo out of the ER.

The Vma21p/V_0 Complex Is Packaged into COPII-coated Vesicles

We used a well-characterized in vitro assay that recapitulates ER export to determine if Vma21p is packaged into COPII-coated vesicles (Shimoni and Schekman, 2002). Briefly, microsomal membranes were purified from cell extracts and were combined with purified COPII proteins to generate ER-derived transport vesicles. Total and vesicle fractions were collected and then analyzed by SDS-PAGE and Western blotting.

In Figure 4A, microsomal membranes from cells expressing Vma21p-HA or Vma12p-HA were used in our in vitro ER-export assay. Packaging of Sec61p, the major subunit of the translocon and an ER-resident protein, served as a negative control. Almost no Sec61p could be detected in the vesicle fraction generated from either source of microsomal membranes. In contrast, Sec22p, an R-SNARE that cycles between the ER and Golgi, was efficiently captured into COPII-coated vesicles. Vma21p-HA was easily detected in the COPII-coated vesicle fraction, but was packaged less efficiently than Sec22p. Unlike Vma21p-HA, Vma12p-HA was barely detectable in the vesicle fraction. This finding is consistent with a primary role for Vma12p in the biogenesis of Vph1p, a role that is restricted to the ER.

Having found that Vma21p could be packaged into COPII-coated vesicles in vitro, we wanted to know if the complex containing Vma21p and the fully assembled V_0 sector

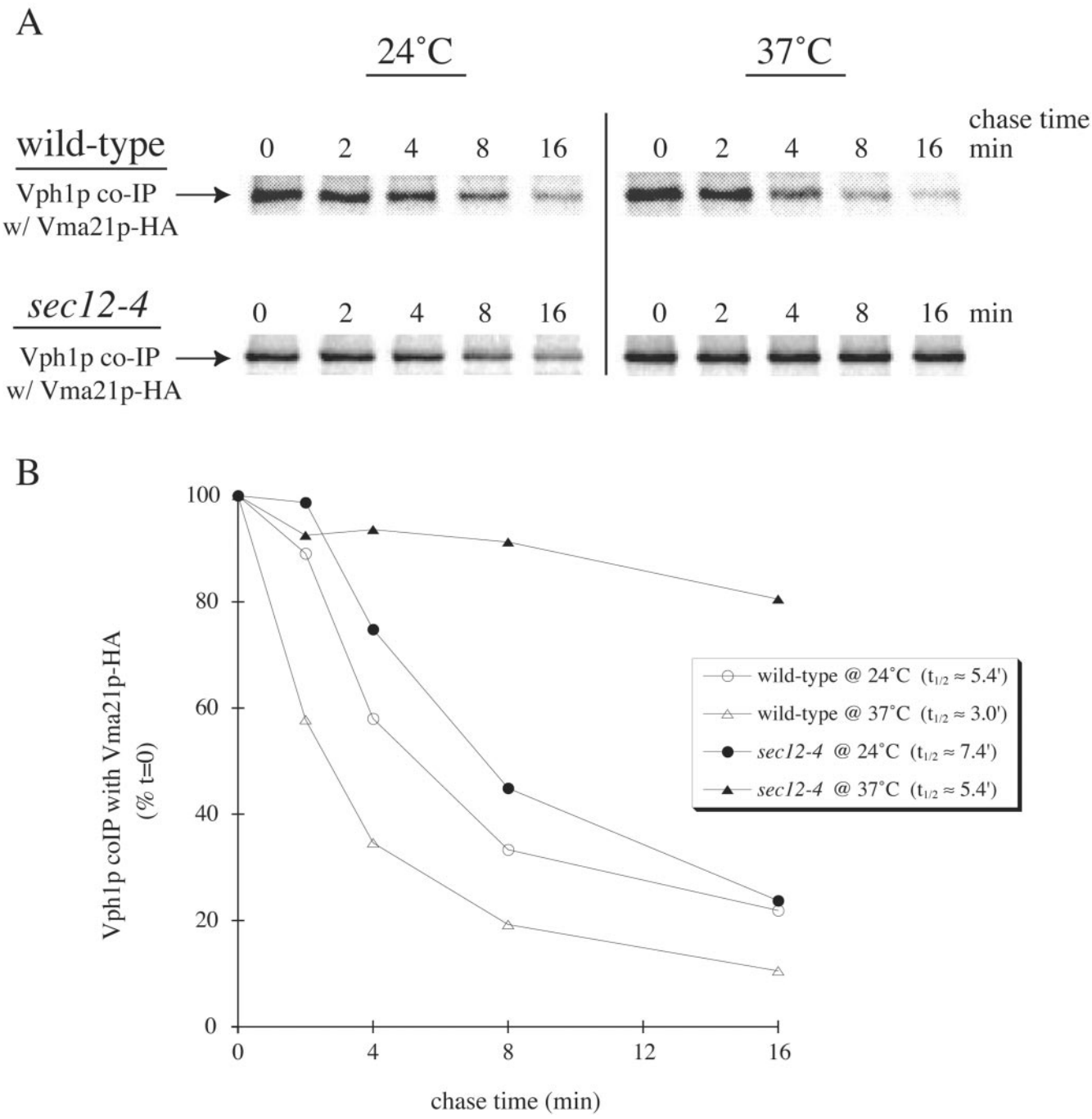

Figure 3. The interaction between Vma21p and V_0 is transient, but can be stabilized by blocking ER export. (A) Wild-type (RSY250/pKH28) and *sec12-4* (RSY263/pKH28) strains expressing Vma21p-HA were grown at 24°C to midlog growth phase and then shifted to the indicated temperature 5 min before the addition of [^{35}S]methionine. Cells were metabolically labeled for 5 min and then an excess of nonradioactive amino acids was added. At the indicated times during the chase period, aliquots were withdrawn and placed on ice. After all samples were collected, membrane extracts were prepared and analyzed by nondenaturing immunoprecipitation as described in Figure 2A. The 100-kDa subunit coimmunoprecipitated with Vma21p-HA is shown. (B) The data in A were quantified and are expressed as a percentage of the band intensity at $t = 0$ of the chase period for each strain and condition tested.

(see Figure 2A) was preferentially taken-up into COPII-coated vesicles. Unfortunately, the microsomal membranes used in the ER-export assay described above are heavily contaminated with vacuolar membranes, which are the primary cellular location of V_0 subunits. Therefore, we turned to an ER-export assay that measures only the packaging of newly synthesized proteins into COPII-coated vesicles (Kuehn *et al.*, 1996). Cells were grown to midlog phase and labeled with [^{35}S]methionine for 3 min. Sodium azide was then added to arrest metabolic activity and, thus, prevent the ER export of membrane proteins that had incorporated radiolabeled amino acids during their synthesis. After con-

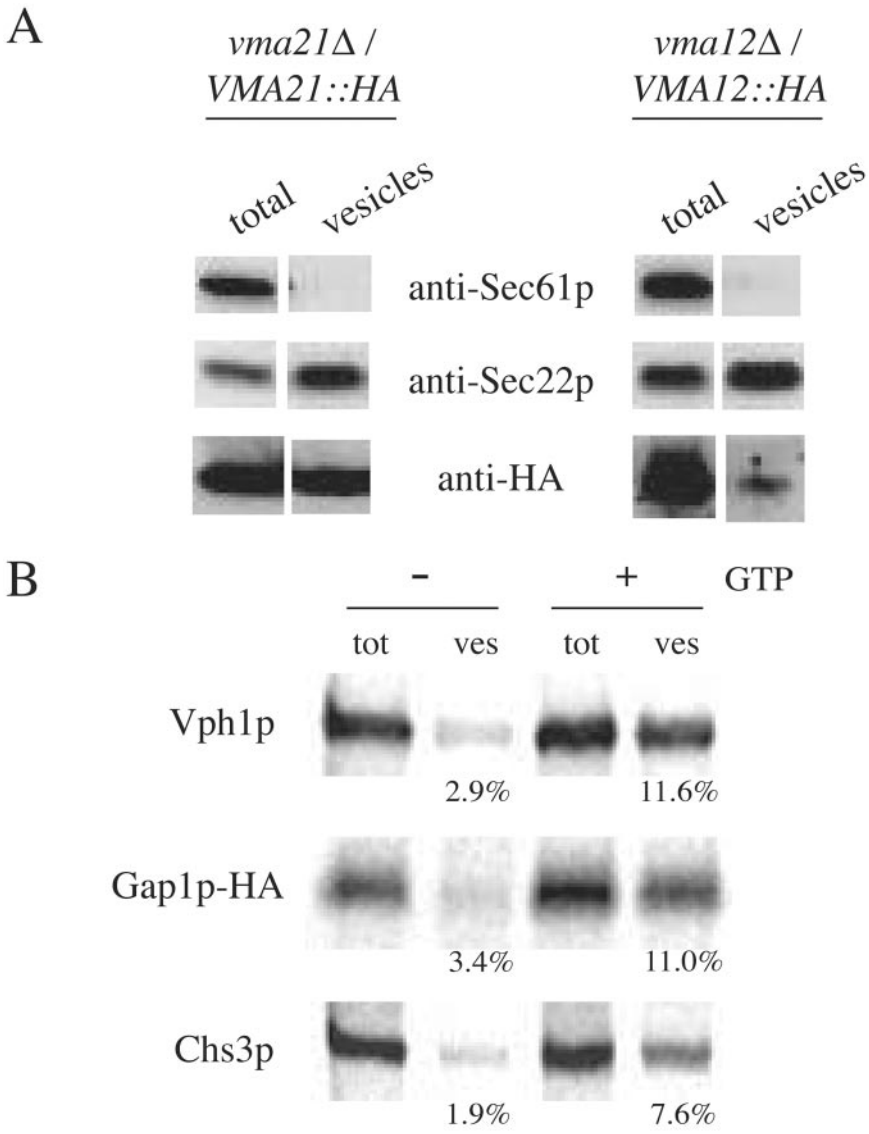

Figure 4. Vma21p and Vph1p are packaged into COPII-coated vesicles. (A) Microsomal membranes prepared from cells expressing either Vma21p-HA or Vma12p-HA were incubated with GTP, and COPII proteins at 25°C for 30 min. Total (10%) and vesicle (60%) fractions were collected and analyzed by SDS-PAGE and Western blotting. (B) Wild-type cells expressing Gap1p-HA were radiolabeled with [^{35}S]methionine for 3 min (or 10 min for experiments with Chs3p) and then arrested by the addition of sodium azide. Cells were converted to spheroplasts and gently lysed to create semi-intact cells (SICs). These membranes were combined with COPII proteins and GTP and incubated at 25°C for 30 min. Total (10%) and vesicle (50%) fractions were collected, solubilized in 1% SDS, and used in immunoprecipitations with anti-Vph1p, anti-HA, and anti-Chs3p antibodies. Immune complexes were resolved by SDS-PAGE and analyzed with a phosphorimager. The percentage of protein recovered in the vesicle fraction is indicated.

verting cells to spheroplasts, we gently ruptured the plasma membrane to yield semi-intact cells (SICs), and these were used for in vitro ER-export reactions, similar to those described in Figure 4A. Radiolabeled proteins were recovered by immunoprecipitation, resolved by SDS-PAGE, and analyzed with a phosphorimager.

We first sought to determine if this assay could faithfully measure Vph1p packaging into COPII-coated vesicles. As shown in Figure 4B (top panel), radiolabeled Vph1p was released into the vesicle fraction (11.6% of total) when COPII proteins and GTP were present in the ER-export assay. GTP is required to activate the small GTP-binding protein, Sar1p, which is a component of the COPII budding machinery (Barlowe *et al.,* 1993). In control reactions lacking GTP, only 2.6% of radiolabeled Vph1p was taken-up into vesicles. To determine if the ER-export efficiency we observed for Vph1p was similar to that of other known secretory cargo, we analyzed the packaging of Gap1p-HA and Chs3p. We chose these proteins because, like Vph1p, both Gap1p and Chs3p have multiple membrane-spanning segments and depend on ER-localized accessory factors to orchestrate their biogenesis and ER export (Ljungdahl *et al.,* 1992; Trilla *et al.,* 1999). We found that Gap1p-HA was packaged into COPII-coated vesicles with an efficiency similar to that of Vph1p (Figure 4B). In reactions containing GTP, the percentage of total Gap1p-HA in the vesicle fraction was 11.0%. Chs3p was also released into the vesicle fraction in a GTP-dependent manner. The packaging efficiency of Chs3p was slightly lower (7.6%) than that observed for Vph1p and Gap1p. This may be due to the longer labeling time (10 min) required to obtain detectable amounts of Chs3p.

We then used this packaging assay to determine if the Vma21p/V_0 complex is taken-up into COPII-coated vesicles. Total and vesicle fractions, taken from reactions containing COPII proteins and GTP, were solubilized under nondenaturing conditions to preserve the interactions between V_0 constituents. Anti-HA antibodies were used to immunoprecipitate Vma21p-HA and associated molecules (as described in Figure 2A). The results from this experiment are shown in Figure 5A. Consistent with the results in Figure 4A, Vma21p-HA is released into the vesicle fraction. The spectrum of radiolabeled proteins that coimmunoprecipitated with Vma21p-HA was the same in both the total and vesicle fractions; however, the stoichiometry of the these interacting

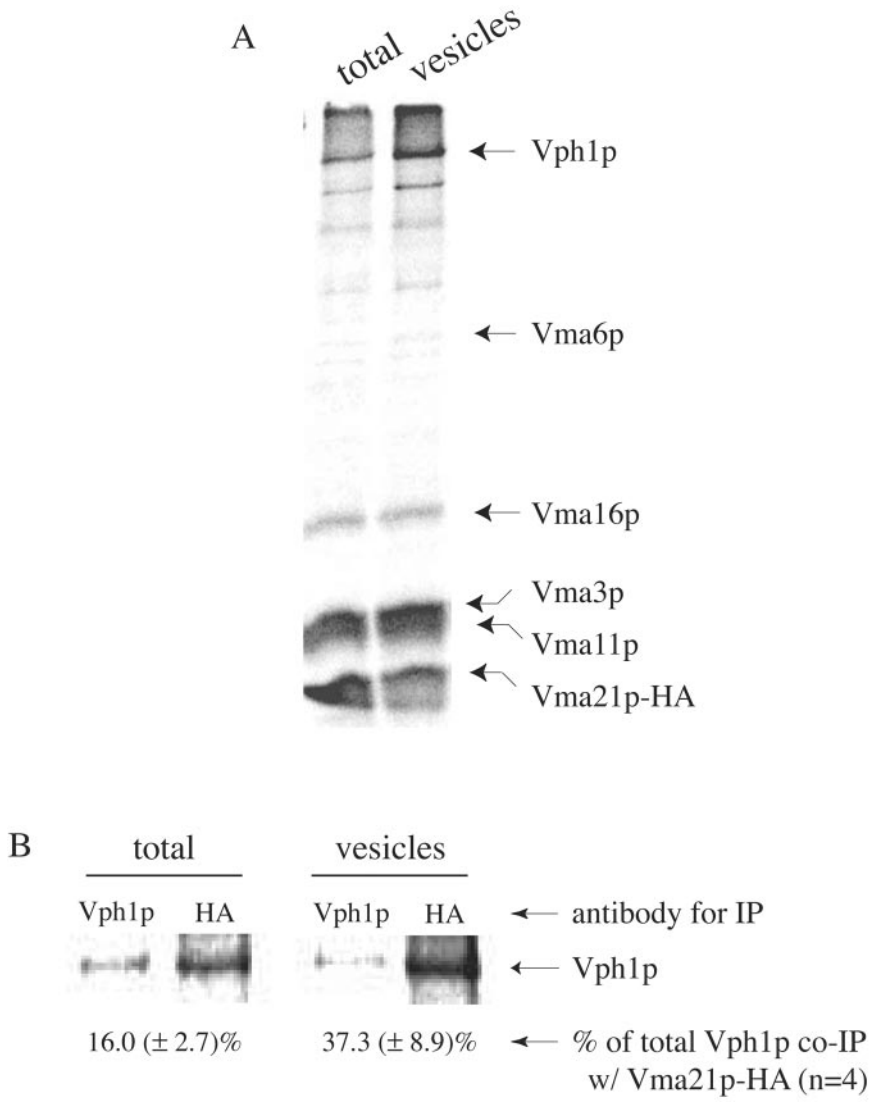

Figure 5. The Vma21p/V_0 complex is enriched in COPII-coated vesicles. (A) Metabolically labeled SICs prepared from *vma21*Δ/*VMA21-HA* cells were used in a COPII-coated vesicle packaging assay as described in Figure 4B. Total (10%) and vesicle (70%) fractions were solubilized in 1% $C_{12}E_9$ and used in immunoprecipitations with anti-HA antibodies. The bound material was separated by SDS-PAGE and analyzed with a phosphorimager. (B) Total and vesicle fractions were generated as in A. The majority (90%) of each fraction was solubilized in 1% $C_{12}E_9$ and used in immunoprecipitations as with anti-HA antibodies. The remaining 10% was solubilized in 1% SDS and used in immunoprecipitations with anti-Vph1p antibodies. Bound material from both immunoprecipitations was resolved by SDS-PAGE and analyzed with a phosphorimager. The amount of Vph1p coimmunoprecipitated with Vma21-HA was determined as a percentage of total Vph1p (Vph1p recovered by denaturing immunoprecipitation).

proteins was different. The amount of proteolipid subunits complexed with Vma21p-HA was similar in both fractions (most clearly seen for Vma16p), whereas the amount of Vph1p coimmunoprecipitated with Vma21p-HA was significantly greater in the vesicle fraction. This suggested that the complex of Vma21p-HA and the fully assembled V_0 sector was preferentially incorporated into COPII-coated vesicles.

To quantify the enrichment of the Vma21p/V_0 complex in vesicles, the percentage of total radiolabeled Vph1p that could be coimmunoprecipitated with Vma21p-HA was determined in both the total and vesicle fractions. ER-export assays using radiolabeled SICs and purified COPII proteins were performed as in Figure 5A. Aliquots (10%) of both the total and vesicle fractions were set aside, and the amount of Vph1p present in these samples was determined by denaturing immunoprecipitation using antibodies against Vph1p. The remaining 90% of the total and vesicle fractions were subjected to nondenaturing immunoprecipitation with anti-HA antibodies. As shown in Figure 5B, ~16% of radiolabeled Vph1p was complexed with Vma21p-HA in the total fraction, whereas ~37% of radiolabeled Vph1p was complexed with Vma21p-HA in the vesicle fraction. Thus, there was a twofold enrichment of the fully assembled Vma21p/V_0 complex in COPII-coated vesicles.

Vma21p Is Required for ER Export of Vph1p In Vitro

If Vma21p plays an active role in directing V_0 subunits into COPII-coated vesicles, these proteins should be inefficiently packaged into vesicles in the absence of Vma21p. To examine this possibility using our in vitro assay, we prepared radiolabeled SICs from wild-type and *vma21*Δ strains. Radiolabeled membranes were also isolated from *vma11*Δ strains, in which Vph1p fails to associate with other V_0 subunits (Figure 1), and from *vma12*Δ strains, in which V_0 subunits still associate, but form an aberrant complex (Figures 1 and 2B). These membranes were used in reactions containing COPII proteins and + or −GTP, and the percentage of Vph1p packaged into COPII-coated vesicles was calculated by comparing total and vesicle fractions, as in Figure 4B. Packaging of Chs3p, whose ER export is independent of *VMA* genes, was measured to control for variations in the activity of membrane preparations from different strains.

As shown in Figure 6 (left panel), packaging of Chs3p into COPII-coated vesicles was GTP dependent and occurred

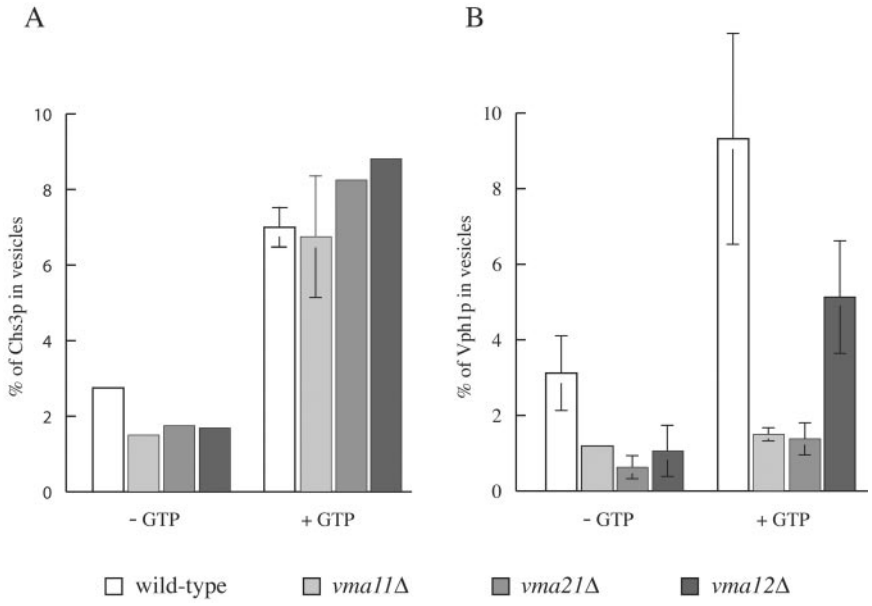

Figure 6. Packaging of Vph1p into COPII-coated vesicles in vitro is dependent on *VMA21*. Radiolabeled membranes were prepared from wild-type, *vma11*Δ, *vma21*Δ, and *vma12*Δ cells and used in packaging assays as described in Figure 4B. Reactions with (+) or without (−) GTP were fractionated and the percentage of total Chs3p (A) or Vph1p (B) released into the vesicle fraction was determined as in Figure 4B.

with efficiency similar to that of wild-type, *vma11*Δ, *vma21*Δ, and *vma12*Δ membranes. ER export of Vph1p was also GTP dependent, but varied greatly depending on the source of membranes. Approximately 9.3% of radiolabeled Vph1p was captured into COPII-coated vesicles from wild-type membranes, whereas packaging of Vph1p from *vma11*Δ and *vma21*Δ membranes measured only ~1.5 and ~1.4%, respectively. Interestingly, packaging of Vph1p from *vma12*Δ membranes was quite efficient (~5.1%). In experiments described in Figure 2A, we observed that Vph1p associates with all five V_0 subunits and with Vma21p in *vma12*Δ cells. Therefore, efficient ER export of Vphp1 may rely primarily on alliance with other V_0 subunits. The poor budding of Vph1p we observed in *vma21*Δ cells could be largely due to a V_0 assembly defect, rather than indicative of a direct role for Vma21p in Vph1p packaging.

Anti-HA Antibodies Diminish Vph1p Budding from Vma21p-HA Membranes

To test whether Vma21p is involved in guiding the assembled V_0 structure into transport vesicles, we attempted to inhibit Vma21p function after V_0 assembly was complete. Membranes were pretreated with antibodies that bind Vma21p and then used in ER-export assays. We anticipated that the antibodies might obscure transport signals present on Vma21p, thereby reducing capture of the assembled V_0 sector in COPII-coated vesicles.

Radiolabeled membranes were prepared from cells possessing an HA-tagged allele of *VMA21* or *VMA12* and from control cells lacking an HA-tagged protein. Before the addition of COPII proteins and GTP, membranes were incubated with anti-HA antibodies or mock treated with BSA. Total and vesicle fractions were isolated from ER-export reactions, and the percentage of Vph1p in the vesicle fraction was calculated. We found that the antibodies had no effect on Vph1p packaging from wild-type or Vma12p-HA membranes (Figure 7A). In contrast, preincubation of Vma21p-HA membranes with anti-HA antibodies resulted in ~37% inhibition of Vph1p packaging into COPII-coated vesicles (Figure 7A). Although modest, this inhibition of Vph1p budding was reproducible and specific to membranes containing Vma21p-HA. Control reactions conducted in parallel also demonstrated that incubation of Vma21p-HA containing membranes with anti-HA antibodies had no effect on packaging of a soluble secretory protein, glycosylated proalpha-factor (gpα-factor; Figure 7B). These results are consistent with the proposal that Vma21p plays a role in guiding the assembled V_0 structure into vesicles that transport cargo out of the ER.

Dissociation of Vma21p-V_0 Precedes Assembly of V_0/V_1

We were intrigued by the possibility that Vma21p could serve another purpose in V-ATPase biogenesis: preventing premature assembly of an enzymatically active V_0/V_1 structure early in the secretory pathway. It is well known that there is a gradient of acidity across the secretory pathway in mammalian cells, with the pH of the ER lumen being neutral (~pH 7.2), the Golgi lumen mildly acidic (pH 7.0–6.2), and secretory granules quite acidic (~pH 5; Kim *et al.*, 1996; Miesenbock *et al.*, 1998; Wu *et al.*, 2000). Acidification of these organelles depends on the action of the V-ATPase; however, the basis of the pH gradient is not well understood (Nishi and Forgac, 2002). In yeast it is presumed that a similar gradient exists along the secretory pathway, but only the pH of the lumen of the vacuole has been measured, and the vacuole lumen was found to be pH ~5.9 (Preston *et al.*, 1989; Plant *et al.*, 1999). One mechanism to establish such a gradient is to limit or prohibit the activity of the V-ATPase in early cellular compartments. Because Vma21p associates with V_0 early in the secretory pathway, we hypothesized that this interaction might prevent assembly of a proton translocating V_0/V_1 structure in the ER and proximal Golgi, thereby reducing the acidity of these organelles.

To explore this possibility, we first compared the kinetics of Vma21p/V_0 dissociation with the kinetics of V_0/V_1 assembly. In the pulse-chase experiment shown in Figure 8 (lanes 1–3) samples from a single culture of *VMA21::HA* cells were split and analyzed by immunoprecipitation for carboxypeptidase Y (CPY; panel 1), Vph1p (panel 2), Vph1p coimmunoprecipitated with Vma21p-HA (panel 3), Vph1p coimmunoprecipitated with Vma1p (the 69-kDa V_1 subunit; panel 4), and Vma2p (the 60-kDa subunit of V_1) coimmuno-

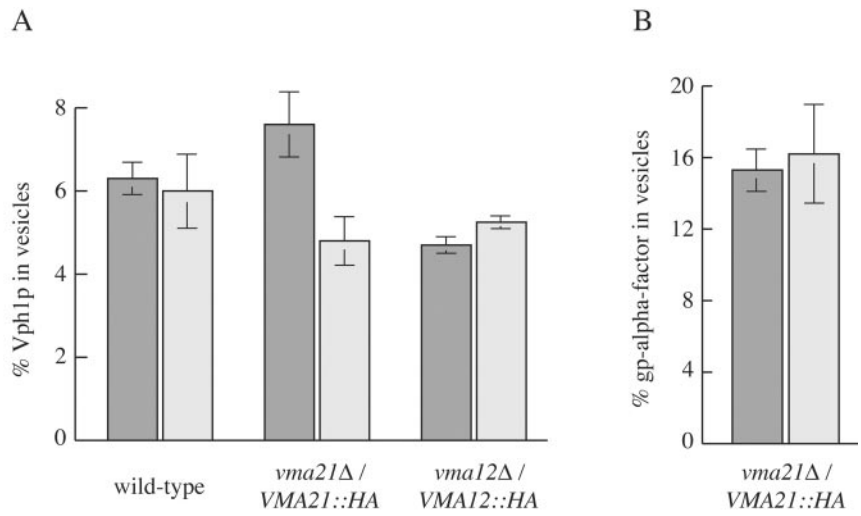

Figure 7. Pretreatment of membranes with antibodies that recognize Vma21p reduces packaging of Vph1p into COPII-coated vesicles. (A) ^{35}S-methionine–labeled SIC membranes were prepared from wild-type (SF838–1Dα), *vma12*Δ/*VMA12::HA,* and *vma21*Δ/*VMA21::HA* cells. Membranes were washed with 1 M KOAc/B88 (see *Materials and Methods*) to remove endogenous COPII proteins and were incubated with 4 μg purified monoclonal anti-HA in 5% BSA/B88 for 2 h at 4°C (light boxes). Mock-treated samples were similarly incubated except that antibody was omitted (dark boxes). Membranes were then washed twice with 0.1% BSA/B88, twice with B88, and used in packaging reactions containing COPII proteins and GTP. The packaging of Vph1p into vesicles was determined as in Figure 4B. (B) ^{35}S-labeled prepro-α-factor, generated by in vitro transcription/translation, was translocated into unlabeled SIC membranes prepared from *vma21*Δ/*VMA21-HA* cells. Membranes were then washed, incubated with antibody, washed again, and used in ER-export reactions, as described in A. The amount of gpα-factor released into the vesicle fraction was determined by scintillation counting.

precipitated with Vma1p (panel 5). As expected, CPY was proteolytically cleaved to a mature form during the course of the chase, indicating that it was transported to the vacuole (Conibear and Stevens, 2002). The total amount of radiolabeled Vph1p did not change substantially (Figure 8, panel 2), whereas the amount of Vph1p associated with Vma21p-HA decreased during the chase period (Figure 8, panel 3). The rate of V_0/V_1 assembly, as assessed by the association of Vph1p (a V_0 subunit) with Vma1p (a V_1 subunit), increased during the chase. Quantification of these data reveals that the rate of Vma21p/V_0 dissociation mirrored the rate of V_0/V_1 assembly, suggesting that Vma21p may free V_0, allowing V_0 to interact with the V_1 sector (Figure 8B).

The data presented in Figure 3 showed that blocking exit from the ER stabilized the interaction between Vma21p and V_0. Once again we used a *sec* mutant, in which transport was conditionally arrested, to determine if stabilization of the Vma21p/V_0 complex affected V_0/V_1 assembly. The right-hand panel of Figure 8A shows a pulse-chase experiment using *sec18–1/VMA21::HA* cells incubated at either 24 or 37°C. In *sec18−1* cells grown at a restrictive temperature (37°C), transport vesicles fail to fuse with acceptor compartments, causing a rapid back-up in the secretory pathway that abrogates ER export (Novick *et al.*, 1981). As shown in Figure 8A (panel 1, lanes 7–12), transport and maturation of CPY occurred normally in *sec18-1/VMA21::HA* cells incubated at 24°C, but was fully eliminated at 37°C. The stability of Vph1p was not significantly affected by either the *sec18* mutation or elevated temperature (Figure 8A, panel 2, lanes 7–12). In keeping with the results of Figure 3, dissociation of Vph1p from Vma21p-HA occurred rapidly in *sec18* cells incubated at 24°C, but was completely blocked at 37°C (Figure 8A, panel 3, lanes 7–12). The amount of Vph1p coimmunoprecipitated with Vma1p increased steadily over the chase period when cells were incubated at 24°C. However, at 37°C, a consistently small amount of Vph1p coimmunoprecipitated with Vma1p, indicating that V_0/V_1 assembly was arrested by incubation of *sec18* cells at 37°C (Figures 8A, panel 4, lanes 7–12, and 8C). Association of V_1 subunits with each other was not affected by the transport block, as demonstrated by uniform coimmunoprecipitation of Vma2p (the 60-kDa subunit of V_1) with Vma1p in both wild-type and *sec18* cells (Figure 8A, panel 5).

Vma21(QQ)p Associates with V_0 in Vacuole, but Does Not Prevent V_0/V_1 Assembly

The data presented in Figure 8 argue that assembly of a V_0/V_1 complex may occur only after the release of the V_0 sector from Vma21p. To further examine this possibility, we made use of a mutant form of Vma21p that is not retrieved to the ER, Vma21(QQ)p (Hill and Stevens, 1994). We asked whether Vma21(QQ)p remains associated with V_0 en route to the vacuole, and if so, whether Vma21(QQ)p/V_0 interaction precludes formation of V_0/V_1 complexes.

First, we determined whether Vma21(QQ)p remains associated with the V_0 subcomplex after leaving the ER. To do this, we performed a pulse-chase experiment comparing the half-life of the interaction between the V_0 100-kDa subunit and wild-type or mutant Vma21p. *vma21*Δ cells expressing either Vma21p-HA or Vma21(QQ)p-HA were incubated for a brief time in the presence of radiolabel, followed by a 60-min incubation in the presence of excess unlabeled amino acids. Vma21p-HA and Vma21(QQ)p-HA were immunoprecipitated under nondenaturing conditions using an anti-HA antibody and analyzed using SDS-PAGE for coimmunoprecipitation of the 100-kDa V_0 subunit. As shown in Figure 9A, very little 100-kDa subunit was coimmunoprecipitated with Vma21p after the 60-min chase, indicating that wild-type Vma21p interacts transiently with the 100-kDa V_0 subunit. In contrast, the interaction between mutant Vma21p(QQ) and V_0 was long-lived and did not appear to decrease after the 60-min chase period, suggesting that most of the newly synthesized 100-kDa subunit remains bound to Vma21p(QQ) even after V_0 assembly is complete. However, this type of experiment does not tell us where in the cell the Vma21(QQ)p/V_0 interaction occurs and whether these complexes are present on the vacuole or only en route to the vacuole?

We wanted to determine how much of the Vma21(QQ)p present on the vacuole interacts with the V_0 subcomplex and if this continued interaction prevents V_0/V_1 assembly. Vacuolar membranes from cells expressing wild-type or mutant Vma21p were isolated, solubilized, and fractioned to determine if vacuolar Vma21p(QQ) cofractionates with V_0 subunits and/or with V_0/V_1 complexes. Consistent with previously published immunolocalization of Vma21(QQ)p,

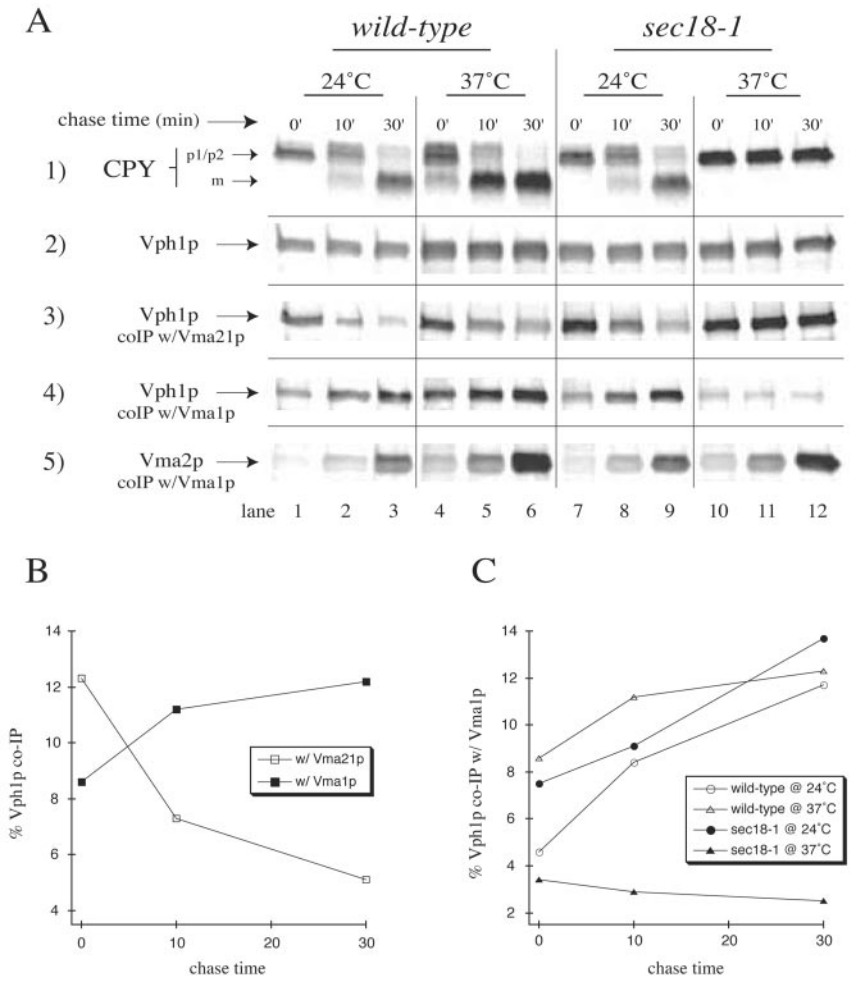

Figure 8. Blocking secretion stabilizes the Vma21p/V_0 complex and prevents V_0/V_1 assembly. (A) Wild-type (RSY250/pKH28) and *sec18-1* (RSY271/pKH28) strains expressing Vma21p-HA were grown at 24°C and then shifted to the indicated temperature for 5 min before metabolic labeling (10-min pulse). The chase period was initiated by the addition of an excess of nonradioactive amino acids, and aliquots were withdrawn at 0, 10, and 30 min. Samples were lysed, and membrane extracts were prepared. Carboxypeptidase Y (CPY; panel 1) and Vph1p (panel 2) were recovered by immunoprecipitation under denaturing conditions. The remainder of each sample was solubilized in nondenaturing conditions and subjected to immunoprecipitation with anti-HA antibodies (panel 3) or anti-Vma1p antibodies (panels 4 and 5). The amount of Vph1p coimmunoprecipitated with Vma21p-HA and Vma1p is shown in panels 3 and 4, respectively. Assembly of the V_1 sector was assessed by coimmunoprecipitation of Vma2p with Vma1p (panel 5). (B) The rate of Vph1p dissociation from Vma21p-HA is compared with the rate of Vph1p association with Vma1p (Quantitation of panels 3 and 4, lanes 4–6). (C) The rate of Vph1p association with Vma1p at 24 and 37°C in wild-type and *sec18-1* cells is compared (quantitation of panel 4).

considerably more of the mutant Vma21p was present on the vacuole compared with wild-type Vma21p (Figure 9B; compare the 3rd and 6th panels). As anticipated, a very low level of wild-type Vma21p was detected in fractions 4 and 5, and very likely represents contamination of the enriched vacuolar membranes with ER membranes (Jackson and Stevens, 1997). Both V_0 and V_1 subunits were detected in fractions 7–11, indicating that these fractions contain fully assembled V-ATPase complexes (V_0/V_1). The low level of wild-type Vma21p did not cofractionate with the V_0/V_1 complex fractions, consistent with its presence in the vacuole-enriched sample due to contaminating ER membranes. A large proportion of the Vma21(QQ)p present in the vacuole (fractions 2–4) did not cofractionate with the V_0/V_1 containing fractions (7–11). This free Vma21(QQ)p may represent protein that has already dissociated from V_0 subunits or Vma21(QQ)p that escaped the ER without being associated with V_0 cargo. Importantly, at least some of the Vma21(QQ)p localized on the vacuole cofractionated with V_0/V_1 complexes (fractions 7–11), suggesting a direct interaction between Vma21(QQ)p and V_0/V_1 complexes on the vacuole.

To confirm whether Vma21(QQ)p is physically associated with the fully assembled V-ATPase complex on the vacuole membrane, we immunoprecipitated Vma21(QQ)p-HA from solubilized vacuole membranes and determined whether V_0 and V_1 subunits coprecipitated. Vacuole membranes were solubilized in 1% $C_{12}E_9$ and Vma21(QQ)p-HA precipitated with anti-HA polyclonal antibodies. The immunoprecipitated proteins were subjected to SDS-PAGE, and blots were probed with anti-HA monoclonal, anti-Vph1p (V_0 subunit), and anti-Vma2p (V_1 subunit) antibodies (Figure 9C). The presence of both Vph1p and Vma2p in the anti-HA immunoprecipitate of cells expressing Vma21(QQ)p-HA but not Vma21p indicates that Vma21(QQ)p is directly associated with the fully assembled V-ATPase complex on the vacuole membrane. These data indicate that the prolonged association of Vma21(QQ)p with V_0 does not prevent assembly of the V_1 subunits with the V_0 subcomplex to form a fully assembled V-ATPase complex.

DISCUSSION

The ER is the site of membrane protein biosynthesis and, therefore, possesses a number of resident proteins that assist in the folding, assembly, and transport of newly translated membrane proteins. Some ER-resident chaperones in yeast act on a broad spectrum of targets (e.g., Kar2p, PDI), whereas others facilitate the biosynthesis of only a few substrates (Ellgaard *et al.*, 1999). Although a number of substrate-specific chaperones have been identified, the precise function of these proteins is largely unclear (Herrmann *et al.*, 1999). We sought to understand how three ER-localized accessory factors, (Vma12p, Vma21p, and Vma22p) facilitate biogenesis of the yeast V-ATPase.

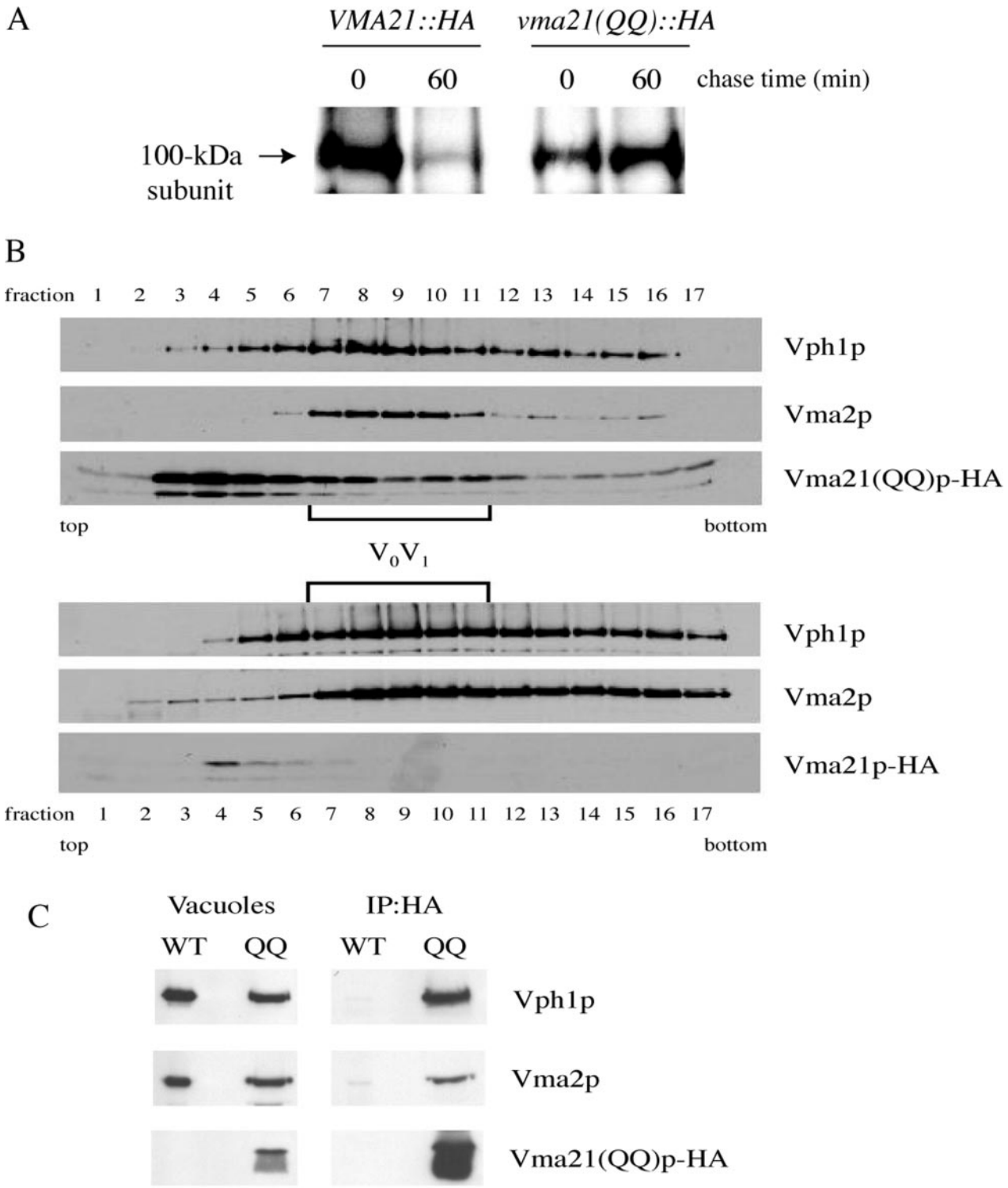

Figure 9. Vma21p(QQ) associates with V_0 in vacuole, but does not prevent V_0V_1 assembly. (A) Cells expressing Vma21p-HA (*vma21*Δ/pKH28) or Vma21(QQ)p-HA (*vma21*Δ/pKH31) were metabolically labeled for 10 min and then chased for 60 min. Samples collected $t = 0$ and $t = 60$ min of the chase period were solubilized under nondenaturing conditions (1% $C_{12}E_9$) and used in immunoprecipitations with anti-HA antibodies. The 100-kDa V_0 subunit that was coimmunoprecipitated is shown. (B) Vacuoles purified from cells expressing Vma21p-HA (*vma21*Δ/pKH28) or Vma21(QQ)p-HA (*vma21*Δ/pKH31) were solubilized in 1% $C_{12}E_9$ and applied to a 20–50% glycerol gradient, which was centrifuged at 175,000 × *g* for 20 h. Samples were collected from the top and analyzed by SDS-PAGE and Western blotting. (C) Native immunoprecipitation using rabbit anti-HA antibodies from 1% $C_{12}E_9$ solubilized vacuoles purified from either wild-type cells or *vma21*Δ cells expressing Vma21p(QQ)-HA. Immunoprecipitated proteins were separated by SDS-PAGE and analyzed by Western blotting using monoclonal antibodies recognizing either Vph1p, Vma2p, or HA. Ten micrograms of vacuolar membranes or 1/10 of the immunoprecipitation reaction from 1 mg of solubilized vacuolar membranes was loaded per lane.

Role of ER-localized Accessory Proteins in Assembly of the V_0 Sector

Previous work has shown that the major 100-kDa subunit of V_0 (Vph1p) is rapidly degraded in cells lacking either a V_0 subunit or one of the V-ATPase accessory factors. It has been proposed that Vph1p instability in *vma* mutants is a result of a V_0 assembly defect (Graham *et al.*, 2003). We tested this possibility by determining whether Vph1p could be coimmunoprecipitated with an HA-tagged version of the proteolipid subunit, Vma3p, in wild-type and *vma* mutant strains. As expected, the majority of Vph1p was complexed with Vma3p-HA in wild-type cells. In cells lacking the proteolipid subunit Vma11p or the peripheral subunit Vma6p, Vph1p failed to interact with Vma3p-HA. A striking defect in the association of Vph1p and Vma3p-HA was also observed in *vma21*Δ cells. Thus, one clear role for Vma21p in V-ATPase biogenesis is simply to bring the subunits of V_0 together.

In *vma12*Δ and *vma22*Δ cells, Vph1p stability is severely comprised, yet Vph1p still associated with Vma3p-HA and other V_0 subunits. This surprising result shows that a careful distinction must be made between association/interaction of V_0 subunits and productive assembly of a V_0 sector. Association of V_0 subunits alone is not sufficient to create a functional V_0 sector, nor is it sufficient to prevent Vph1p degradation.

It is possible that Vph1p is misfolded in *vma12*Δ and *vma*Δ*22* cells such that it still interacts with other V_0 subunits, but is nonetheless targeted for rapid degradation. Previous analysis of the folded state of Vph1p by partial proteolysis yielded identical patterns when microsomes from wild-type and *vma*Δ*12* cells were exposed to protease (Jackson and Stevens, 1997), suggesting no dramatic changes in the overall structure of the large N-terminal cytosolic domain of Vph1p. If Vph1p is misfolded in *vma12*Δ cells (and presumably *vma22*Δ cells), the effect must be subtle, because it still associates with other V_0 subunits in the ER yet the complex formed is not competent for assembly with V_1 or for transport to the vacuole.

More recent results provide evidence that in *vma12*Δ and *vma22*Δ cells Vph1p is degraded by a proteasomal pathway devoted to the removal of misfolded cytosolic proteins. Hill and Cooper found that *UBC6* and *UBC7*, genes encoding ubiquitin conjugating enzymes required for degradation of misfolded integral membrane proteins, were not needed for degradation of Vph1p in *vma22*Δ cells (Hill and Cooper, 2000). Instead, *UBC1* and *UBC4*, two genes required for degradation of short-lived cytosolic proteins, influenced the rate of Vph1p degradation in *vma22*Δ cells. Furthermore, they found that cytosolic (Ssa1p), rather than lumenal (Kar2p), chaperones were involved in Vph1p delivery to the proteasome in *vma22*Δ cells. Curiously, other studies have shown that rapid degradation of Vph1p in *vma21*Δ cells depends on *UBC6* and *UBC7* as well as components of the ERAD machinery (Hrd1p; Wilhovsky *et al.*, 2000). At the time these data appeared contradictory, and the authors did not comment on the inconsistency between *vma22*Δ and *vma21*Δ strains. Given the results of Figures 1 and 2, it seems likely that Vph1p is in different assembly states in *vma22*Δ and *vma21*Δ cells and that this difference may influence the pathway that Vph1p takes to the proteasome. Therefore, we reason that Vma12p/Vma22p may be required for proper folding of the large cytosolic amino-terminal domain of Vph1p.

The absence of Vma21p from the Vma12p/Vma22p/Vph1p assembly complex suggests that Vma21p is involved in a parallel pathway (interacting with the proteolipid subunits) or in a downstream pathway (interacting with both Vph1p and other V_0 subunits; Graham *et al.*, 1998). To explore this question, we asked what V_0 subunits interacted with Vma21p-HA. We found that all five V_0 subunits were specifically coimmunoprecipitated with Vma21p-HA. The interaction between Vma21p-HA and V_0 was transient, reflecting the different cellular localizations of Vma21p and V_0. Furthermore, blocking export of newly synthesized proteins out of the ER stabilized the interaction between Vma21p-HA and V_0.

We used *vma*Δ strains to determine which V_0 subunits interact directly with Vma21p-HA and which V_0 subunits associate with Vma21p-HA through other V_0 subunits. We found that in *vma3*Δ and *vma16*Δ strains, the remaining two proteolipid subunits retained the ability to interact with Vma21p-HA, but Vma6p and Vph1p did not. In *vma11*Δ strains, no V_0 subunits coimmunoprecipitated with Vma21p-HA. This suggests that Vma11p serves as the link that connects Vma21p-HA to V_0. Vma21p is only 8.5-kDa, consisting of two transmembrane domains, a 12-residue lumenal loop, and N- and C- terminal cytosolic domains of 12 and 16 residues, respectively. It is somewhat remarkable that such a small molecule can coordinate the assembly of the ~240-kDa V_0 sector, and it would be even more remarkable if it made contacts with each V_0 subunit. Instead, Vma21p seems to interact with V_0 via a single subunit, Vma11p.

The analysis of *vma*Δ strains also suggests that Vma6p and Vph1p can only interact with Vma21p when all the proteolipid subunits are present. Although Vma6p coimmunoprecipitated with Vma21p-HA in *vph1*Δ cells, Vph1p was absent from Vma21p-HA/proteolipid complexes in *vma6*Δ cells. Thus, Vph1p can only associate with Vma21p-HA when all other V_0 subunits are present. Together these observations suggest that Vma21p serves as a nucleation point around which V_0 assembly takes place and that Vph1p is the last subunit added to form a completed V_0 sector (Figure 10).

Transport of the Assembled V_0 Sector out of the ER

The carboxy-terminal region of Vma21p contains a −KKXX sequence that is required for localization of Vma21p to the ER. Mutation of this sequence to −QQXX results in a protein, Vma21p-QQ, that accumulates in the vacuole (Hill and Stevens, 1994). Many studies have shown that carboxy-terminal −KKXX sequences are directly recognized by components of the COPI coat and that binding leads to inclusion of −KKXX containing proteins into COPI-coated transport vesicles that travel from the Golgi toward the ER (Wieland and Harter, 1999). The presence of a bona fide ER-retrieval signal in Vma21p suggests that Vma21p escorts the assembled V_0 sector to the Golgi.

We used a well-established in vitro assay to examine the role of Vma21p in ER export of V_0. Preliminary experiments showed that Vma21p-HA, but not Vma12p-HA, was packaged into ER-derived transport vesicles. This finding is consistent with the proposed role for Vma12p in facilitating folding of the amino-terminal domain of Vph1p, which most likely occurs in the ER during translation. Subsequent experiments examined packaging of Vma21p-containing protein complexes into COPII-coated vesicles. We found that the complex of Vma21p-HA and the fully assembled V_0 sector was enriched approximately twofold in ER-derived vesicles. This suggests that ER export of V_0 subunits is suspended until V_0 assembly is complete and that Vma21p accompanies the V_0 sector to the Golgi. This is the first demonstration of enrichment into ER-derived vesicles of a

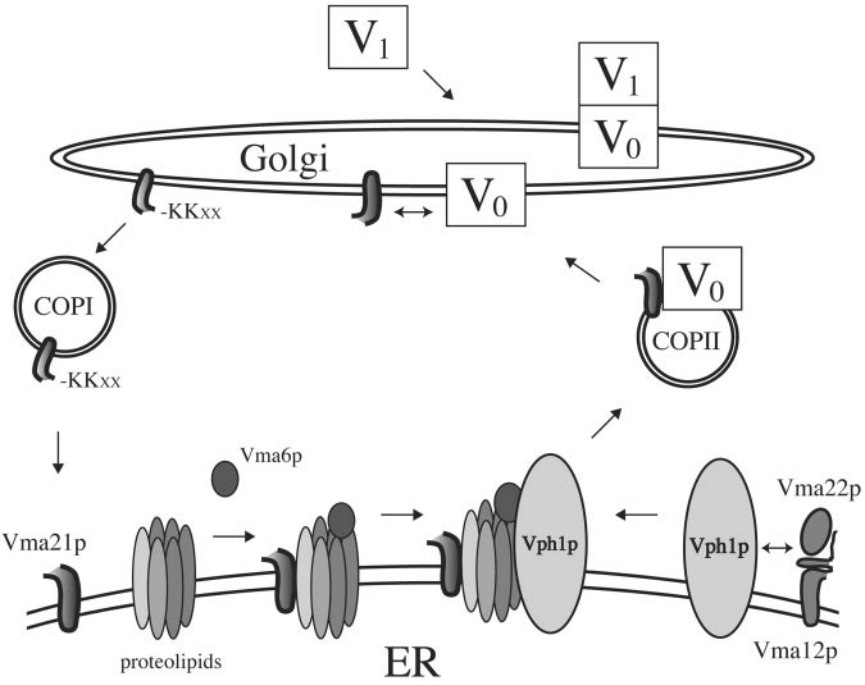

Figure 10. A model for assembly and transport of the yeast V-ATPase. The Vma12p/Vma22p complex interacts transiently with newly synthesized Vph1p, perhaps aiding in folding the large cytosolic amino-terminal domain of this 100-kDa subunit. In a parallel pathway, Vma21p associates with the proteolipid subunits of V_0, Vma3p/Vma11p/Vma16, and subsequently with Vma6p, a peripheral membrane protein. V_0 assembly proceeds only when all four proteins, Vma3p/Vma11p/Vma16p/Vma6p, have bound to Vma21p. Thereafter, Vph1p can be transferred from Vma12p/Vma22p to complete assembly of the V_0 sector. Vma21p remains associated with the fully assembled V_0 structure, escorting V_0 into COPII-coated vesicles that bud from the ER. The Vma21p/V_0 complex is enriched in COPII-coated vesicles, but dissociates rapidly after arriving at the Golgi. The free V_0 sector associates with the cytosolic V_1 sector, allowing formation of an enzymatically active V-ATPase consisting of coupled V_0V_1 sectors. Vma21p is returned to the ER in COPI-coated vesicles where it can participate in another round of V_0 biogenesis.

complex containing a transmembrane cargo complex (V_0) and an accessory protein (Vma21p). Other studies have presented evidence for a physical interaction between a cargo protein and an accessory protein, but none of these studies showed preferential incorporation of a cargo-accessory complex into COPII-coated vesicles (Gas1p/p24, Muniz *et al.*, 2000; SREBP/SCAP, Nohturfft *et al.*, 2000; and gpα-factor, Erv29p, Belden and Barlowe, 2001), Axl2p/Erv14p, Powers and Barlowe, 2002). Importantly, several of these studies did demonstrate that specific amino acid sequences in the accessory protein were required for ER export of both cargo and escort. We have yet to identify such sequences in Vma21p.

To determine if Vma21p contains information required for ER export of the assembled V_0 sector, we first examined packaging of Vph1p into COPII-coated vesicles in *vma21*Δ strains. Using our in vitro assay, we showed that ER export of Vph1p from *vma21*Δ membranes is about six times less efficient than from wild-type membranes. A similar defect in Vph1p packaging was observed when *vma11*Δ membranes were used. We showed in Figure 1 that both Vma21p and Vma11p are required for Vph1p to associate with other V_0 subunits. Therefore, inefficient packaging of Vph1p in *vma21*Δ cells is most likely due to an assembly defect, rather than a direct role for Vma21p in Vph1p transport from the ER.

Interestingly, ER export of Vph1p from *vma12*Δ membranes was about three times more efficient than from *vma21*Δ or *vma11*Δ membranes. We found that Vph1p still associates with other V_0 subunits and with Vma21p in *vma12*Δ cells (Figures 1 and 2B). This indicates that oligomerization of V_0 subunits may be one factor that promotes V_0 packaging. Individually, V_0 subunits may display weak ER-export signals, that when brought together into a V_0 sector, provide a sufficient impetus for inclusion into COPII-coated vesicles. Oligomerization has also been implicated in regulating transport of ERGIC-53 (Appenzeller *et al.*, 1999), Erv41p/Erv46p (Otte and Barlowe, 2002), and Emp24p/Erv25p (Belden and Barlowe, 1996).

To address the role of Vma21p in ER export of a properly assembled V_0 sector, we tried to inhibit Vma21p function in wild-type membranes using antibodies. In these experiments, pretreatment of membranes with antibodies that recognize Vma21p reduced the ER export of Vph1p by ~37%. Although, this effect was modest, it was reproducible, specific to Vph1p (gpα-factor packaging was unaffected) and specific to membranes expressing an epitope-tagged Vma21p molecule recognized by the antibodies. We propose that the bound antibody obscured a transport signal required for efficient ER export of Vma21p/V_0. It is unclear whether this transport signal is present on Vma21p or on an adjacent V_0 subunit that might have also been obscured by bound antibody. To convincingly demonstrate a postassembly role for Vma21p in V_0 transport, we are attempting to generate a Vma21p mutant, where assembly and transport functions are uncoupled.

Dissociation of Vma21p-V_0 Complex and Assembly of V_0/V_1

We wondered whether Vma21p might also serve a regulatory function, preventing premature assembly of a proton-pumping V_0/V_1 complex early in the secretory pathway. In so doing, Vma21p could contribute to the maintenance of neutral pH in the ER and *cis*-Golgi compartments. Previous work has shown that coimmunoprecipitation of Vph1p (a V_0 subunit) with Vma1p (a V_1 subunit) is reduced in *sec18-1* cells incubated at a restrictive temperature (Kane *et al.*, 1999). Surprisingly, the authors did not interpret this as evidence that V_0/V_1 complexes fail to assemble when transport from the ER is blocked. We extended their analysis by comparing the kinetics of Vma21p-HA/V_0 dissociation to the kinetics of V_0/V_1 assembly in wild-type and *sec18-1* cells. Pulse-chase experiments showed that the rate of Vma21p-HA/V_0 dissociation mirrored the rate of V_0/V_1 assembly. Furthermore, blocking vesicle traffic arrested both dissociation of Vma21p/V_0 and assembly of V_0/V_1. Our results indicate that V_0/V_1 cannot assemble on the ER membrane and that

the interaction of Vma21p with V_0 in early cellular compartments may block V_0/V_1 assembly.

To explore this possibility, we analyzed Vma21p/V_0 dissociation and V_0/V_1 assembly in strains expressing a retrieval-defective Vma21p mutant, Vma21(QQ)p. Vma21(QQ)p was found to remain associated with V_0 because both proteins transited the secretory pathway to the vacuole and in the vacuole as well. Surprisingly, the prolonged association of Vma21(QQ)p with the V_0 subcomplex did not appear to have a significant effect on V_0/V_1 assembly. Gradient fractionation of vacuoles from strains expressing Vma21(QQ)p suggested that Vma21(QQ)p interacts with both free V_0 sectors as well as assembled V_0/V_1 structures, and coprecipitation of V_1 and V_0 subunits with Vma21(QQ)p from vacuole membranes confirmed the direct association. Therefore, it seems unlikely that Vma21p prevents assembly of V_0/V_1 in the ER or in downstream compartments. It may be that the interaction between Vma21p and V_0 is highly dynamic, moving rapidly between bound and unbound states. In the ER, Vma21p is abundant and Vma21p/V_0 complexes could be favored, to the exclusion of V_0/V_1 complexes. In contrast, the concentration of Vma21p molecules in the Golgi is low, and dissociation of Vma21p/V_0 complexes could result in a greater population of free V_0 sectors that are then competent to assemble with the V_1 sector. Once formed, V_0/V_1 complexes could be relatively stable and not perturbed by the presence of Vma21p.

Vma21p Homologues

Given the crucial role that Vma21p plays in biogenesis of the V_0 sector in *S. cerevisiae*, one would expect to find functional counterparts of Vma21p in other organisms that rely on V-ATPases to carry out fundamental cellular processes. An extensive group of small hydrophobic proteins of molecular mass 9.2–9.4 kDa have been identified that are similar in primary sequence to Vma21p and that are predicted to span the membrane twice. Vma21p-like proteins have been identified in the genomes of all eukaryotic organisms sequenced to date. Yeast Vma21p (NP_011619) shows ~21–25% identity to proteins in *Arabidopsis* (NP_565728), *C. elegans* (CAA83627), *Drosophila* (AAF51611), and humans (XP_377060). The Vma21 proteins from fungi and plants have a carboxy-terminal dilysine motif, suggesting they are ER localized and may function in V-ATPase assembly similar to the yeast Vma21p. Unlike the Vma21 proteins from fungi and plants, the metazoan Vma21 proteins lack a carboxy-terminal dilysine and instead have a single lysine at the −3 position and terminate with an acidic aspartate residue (XKXD). Further analysis of the metazoan homologues may provide insights into whether they are ER localized and function in V-ATPase assembly.

ACKNOWLEDGMENTS

This work was supported by the Howard Hughes Medical Institute and by grants from the National Institutes of Health (GM26755 and GM38006) to R.S. and T.H.S., respectively.

REFERENCES

Appenzeller, C., Andersson, H., Kappeler, F., and Hauri, H.P. (1999). The lectin ERGIC-53 is a cargo transport receptor for glycoproteins. Nat. Cell Biol. *1*, 330–334.

Ausubel, F.M., Brent, R., Kingston, R.E., Moore, D.D., Seidman, J.G., Smith, J.A., and Struhl, K. (eds.) (1987). Current Protocols in Molecular Biology, New York: John Wiley & Sons.

Bachhawat, A.K., Manolson, M.F., Murdock, D.G., Garman, J.D., and Jones, E.W. (1993). The VPH2 gene encodes a 25 kDa protein required for activity of the yeast vacuolar H(+)-ATPase. Yeast *9*, 175–184.

Barlowe, C., d'Enfert, C., and Schekman, R. (1993). Purification and characterization of SAR1p, a small GTP-binding protein required for transport vesicle formation from the endoplasmic reticulum. J. Biol. Chem. *268*, 873–879.

Bauerle, C., Ho, M.N., Lindorfer, M.A., and Stevens, T.H. (1993). The *Saccharomyces cerevisiae* VMA6 gene encodes the 36-kDa subunit of the vacuolar H(+)-ATPase membrane sector. J. Biol. Chem. *268*, 12749–12757.

Belden, W.J., and Barlowe, C. (1996). Erv25p, a component of COPII-coated vesicles, forms a complex with Emp24p that is required for efficient endoplasmic reticulum to Golgi transport. J. Biol. Chem. *271*, 26939–26946.

Belden, W.J., and Barlowe, C. (2001). Role of Erv29p in collecting soluble secretory proteins into ER-derived transport vesicles. Science *294*, 1528–1531.

Bowers, K., Levi, B.P., Patel, F.I., and Stevens, T.H. (2000). The sodium/proton exchanger Nhx1p is required for endosomal protein trafficking in the yeast *Saccharomyces cerevisiae*. Mol. Biol. Cell *11*, 4277–4294.

Chuang, J.S., and Schekman, R.W. (1996). Differential trafficking and timed localization of two chitin synthase proteins, Chs2p and Chs3p. J. Cell Biol. *135*, 597–610.

Conibear, E., and Stevens, T.H. (2002). Studying yeast vacuoles. Methods Enzymol. *351*, 408–432.

Doherty, R.D., and Kane, P.M. (1993). Partial assembly of the yeast vacuolar H(+)-ATPase in mutants lacking one subunit of the enzyme. J. Biol. Chem. *268*, 16845–16851.

Ellgaard, L., Molinari, M., and Helenius, A. (1999). Setting the standards: quality control in the secretory pathway. Science *286*, 1882–1888.

Graham, L.A., Flannery, A.R., and Stevens, T.H. (2003). Structure and assembly of the yeast V-ATPase. J. Bioenerg. Biomembr. *35*, 301–312.

Graham, L.A., Hill, K.J., and Stevens, T.H. (1998). Assembly of the yeast vacuolar H+-ATPase occurs in the endoplasmic reticulum and requires a Vma12p/Vma22p assembly complex. J. Cell Biol. *142*, 39–49.

Herrmann, J.M., Malkus, P., and Schekman, R. (1999). Out of the ER—outfitters, escorts and guides. Trends Cell Biol. *9*, 5–7.

Hill, K., and Cooper, A.A. (2000). Degradation of unassembled Vph1p reveals novel aspects of the yeast ER quality control system. EMBO J. *19*, 550–561.

Hill, K.J., and Stevens, T.H. (1994). Vma21p is a yeast membrane protein retained in the endoplasmic reticulum by a di-lysine motif and is required for the assembly of the vacuolar H(+)-ATPase complex. Mol. Biol. Cell *5*, 1039–1050.

Hill, K.J., and Stevens, T.H. (1995). Vma22p is a novel endoplasmic reticulum-associated protein required for assembly of the yeast vacuolar H(+)-ATPase complex. J. Biol. Chem. *270*, 22329–22336.

Hirata, R., Graham, L.A., Takatsuki, A., Stevens, T.H., and Anraku, Y. (1997). VMA11 and VMA16 encode second and third proteolipid subunits of the *Saccharomyces cerevisiae* vacuolar membrane H+-ATPase. J. Biol. Chem. *272*, 4795–4803.

Hirata, R., Umemoto, N., Ho, M.N., Ohya, Y., Stevens, T.H., and Anraku, Y. (1993). VMA12 is essential for assembly of the vacuolar H(+)-ATPase subunits onto the vacuolar membrane in *Saccharomyces cerevisiae*. J. Biol. Chem. *268*, 961–967.

Ho, M.N., Hill, K.J., Lindorfer, M.A., and Stevens, T.H. (1993a). Isolation of vacuolar membrane H(+)-ATPase-deficient yeast mutants; the VMA5 and VMA4 genes are essential for assembly and activity of the vacuolar H(+)-ATPase. J. Biol. Chem. *268*, 221–227.

Ho, M.N., Hirata, R., Umemoto, N., Ohya, Y., Takatsuki, A., Stevens, T.H., and Anraku, Y. (1993b). VMA13 encodes a 54-kDa vacuolar H(+)-ATPase subunit required for activity but not assembly of the enzyme complex in *Saccharomyces cerevisiae*. J. Biol. Chem. *268*, 18286–18292.

Inoue, T., Wilkens, S., and Forgac, M. (2003). Subunit structure, function, and arrangement in the yeast and coated vesicle V-ATPases. J. Bioenerg. Biomembr. *35*, 291–299.

Jackson, D.D., and Stevens, T.H. (1997). VMA12 encodes a yeast endoplasmic reticulum protein required for vacuolar H+-ATPase assembly. J. Biol. Chem. *272*, 25928–25934.

Kaiser, C.A., and Schekman, R. (1990). Distinct sets of SEC genes govern transport vesicle formation and fusion early in the secretory pathway. Cell *61*, 723–733.

Kane, P.M. (1995). Disassembly and reassembly of the yeast vacuolar H(+)-ATPase in vivo. J. Biol. Chem. *270*, 17025–17032.

Kane, P.M., Kuehn, M.C., Howald-Stevenson, I., and Stevens, T.H. (1992). Assembly and targeting of peripheral and integral membrane subunits of the yeast vacuolar H(+)-ATPase. J. Biol. Chem. *267*, 447–454.

Kane, P.M., Tarsio, M., and Liu, J. (1999). Early steps in assembly of the yeast vacuolar H+-ATPase. J. Biol. Chem. *274*, 17275–17283.

Kane, P.M., Yamashiro, C.T., and Stevens, T.H. (1989). Biochemical characterization of the yeast vacuolar H(+)-ATPase. J. Biol. Chem. *264*, 19236–19244.

Kim, J.H., Lingwood, C.A., Williams, D.B., Furuya, W., Manolson, M.F., and Grinstein, S. (1996). Dynamic measurement of the pH of the Golgi complex in living cells using retrograde transport of the verotoxin receptor. J. Cell Biol. *134*, 1387–1399.

Kuehn, M.J., Schekman, R., and Ljungdahl, P.O. (1996). Amino acid permeases require COPII components and the ER resident membrane protein Shr3p for packaging into transport vesicles in vitro. J. Cell Biol. *135*, 585–595.

Ljungdahl, P.O., Gimeno, C.J., Styles, C.A., and Fink, G.R. (1992). SHR3, a novel component of the secretory pathway specifically required for localization of amino acid permeases in yeast. Cell *71*, 463–478.

Manolson, M.F., Wu, B., Proteau, D., Taillon, B.E., Roberts, B.T., Hoyt, M.A., and Jones, E.W. (1994). STV1 gene encodes functional homologue of 95-kDa yeast vacuolar H(+)-ATPase subunit Vph1p. J. Biol. Chem. *269*, 14064–14074.

Miesenbock, G., De Angelis, D.A., and Rothman, J.E. (1998). Visualizing secretion and synaptic transmission with pH-sensitive green fluorescent proteins. Nature *394*, 192–195.

Muniz, M., Nuoffer, C., Hauri, H.P., and Riezman, H. (2000). The Emp24 complex recruits a specific cargo molecule into endoplasmic reticulum-derived vesicles. J. Cell Biol. *148*, 925–930.

Nishi, T., and Forgac, M. (2002). The vacuolar (H+)-ATPases—nature's most versatile proton pumps. Nat. Rev. Mol. Cell. Biol. *3*, 94–103.

Nohturfft, A., Yabe, D., Goldstein, J.L., Brown, M.S., and Espenshade, P.J. (2000). Regulated step in cholesterol feedback localized to budding of SCAP from ER membranes. Cell *102*, 315–323.

Novick, P., Ferro, S., and Schekman, R. (1981). Order of events in the yeast secretory pathway. Cell *25*, 461–469.

Otte, S., and Barlowe, C. (2002). The Erv41p-Erv46p complex: multiple export signals are required in trans for COPII-dependent transport from the ER. EMBO J. *21*, 6095–6104.

Plant, P.J., Manolson, M.F., Grinstein, S., and Demaurex, N. (1999). Alternative mechanisms of vacuolar acidification in H(+)-ATPase-deficient yeast. J. Biol. Chem. *274*, 37270–37279.

Powell, B., Graham, L.A., and Stevens, T.H. (2000). Molecular characterization of the yeast vacuolar H+-ATPase proton pore. J. Biol. Chem. *275*, 23654–23660.

Powers, J., and Barlowe, C. (2002). Erv14p directs a transmembrane secretory protein into COPII-coated transport vesicles. Mol. Biol. Cell *13*, 880–891.

Preston, R.A., Murphy, R.F., and Jones, E.W. (1989). Assay of vacuolar pH in yeast and identification of acidification-defective mutants. Proc. Natl. Acad. Sci. USA *86*, 7027–7031.

Schiestl, R.H., and Gietz, R.D. (1989). High efficiency transformation of intact yeast cells using single stranded nucleic acids as a carrier. Curr. Genet. *16*, 339–346.

Sherman, F. (1991). Getting started with yeast. Methods Enzymol. *194*, 3–21.

Shimoni, Y., and Schekman, R. (2002). Vesicle budding from endoplasmic reticulum. Methods Enzymol. *351*, 258–278.

Stevens, T., Esmon, B., and Schekman, R. (1982). Early stages in the yeast secretory pathway are required for transport of carboxypeptidase Y to the vacuole. Cell *30*, 439–448.

Tomashek, J.J., Graham, L.A., Hutchins, M.U., Stevens, T.H., and Klionsky, D.J. (1997). V1-situated stalk subunits of the yeast vacuolar proton-translocating ATPase. J. Biol. Chem. *272*, 26787–26793.

Trilla, J.A., Duran, A., and Roncero, C. (1999). Chs7p, a new protein involved in the control of protein export from the endoplasmic reticulum that is specifically engaged in the regulation of chitin synthesis in *Saccharomyces cerevisiae*. J. Cell Biol. *145*, 1153–1163.

Wieland, F., and Harter, C. (1999). Mechanisms of vesicle formation: insights from the COP system. Curr. Opin. Cell Biol. *11*, 440–446.

Wilhovsky, S., Gardner, R., and Hampton, R. (2000). HRD gene dependence of endoplasmic reticulum-associated degradation. Mol. Biol. Cell *11*, 1697–1708.

Wu, M.M., Llopis, J., Adams, S., McCaffery, J.M., Kulomaa, M.S., Machen, T.E., Moore, H.P., and Tsien, R.Y. (2000). Organelle pH studies using targeted avidin and fluorescein-biotin. Chem. Biol. *7*, 197–209.

Wuestehube, L.J., and Schekman, R.W. (1992). Reconstitution of transport from endoplasmic reticulum to Golgi complex using endoplasmic reticulum-enriched membrane fraction from yeast. Methods Enzymol. *219*, 124–136.

Abbreviations used: COP, coat protein complex; CPY, carboxypeptidase Y; gpα-factor, glycosylated pro-α-factor; SIC, semi-intact cell; V-ATPase, vacuolar-type proton-translocating ATPase; VMA, vacuolar membrane ATPase.